Chem Rev Lett 6 (2023) 183-212

Research Article

Chemical Review and Letters
journal homepage: www.chemrevlett.com
ISSN (online): 2645-4947 (print) 2676-7279

ptimization of the production of Methyl Ester from used cotton Seed Oil: A Statistical Approach using box-behnken design

Abdullateef Jimoh*, Edith .B. Agbaji, Victor .O. Ajibola & Sani Uba

Department of Chemistry, Ahmadu Bello University, Zaria, Kaduna State, Nigeria
**Correspondence: Jimoh Abdullateef, Department of Chemistry, Kogi State College of Education, Ankpa, Kogi State, Nigeria.*

ARTICLE INFO

Article history:
Received 29 August 2022
Received in revised form 10 October 2022
Accepted 12 January 2023
Available online 10 August 2023

Keywords:
Monoalkyl ester
Transesterification
Vegetable oil
Biodiesel
Free Fatty Acids

ABSTRACT

Methyl ester is the name given to monoalkyl esters of vegetable and animal oils. Since methyl ester has fuel properties that are comparable to those of diesel fuel, it is becoming more popular as a substitute fuel for use in diesel engines. The amount of free fatty acids (FFA) in the oil determines how methyl ester is produced. In this study, the titration method was used to calculate the FFA values of the crude cottonseed oil (CCSO) and one-time Used Cottonseed Oil (UCSO), with values 0.56 % and 1.26 %, respectively. The UCSO is transformed into methyl ester by employing a heterogeneous alkali catalyzed transesterification reaction. It involves the addition of methanol to bleach and degummed UCSO in the presence of heterogeneous catalysts CaO-blend derived from calcinated eggshells and coconut shell blend. Reaction variables including the methanol-to-oil ratio, reaction temperature, reaction time and catalyst concentration control the transesterification process. The Box-Behnken design was employed to optimize the aforementioned parameters using the response surface methodology (RSM). Numerous factors that affect the generation of biodiesel have been plotted using the response surface plot and contour plot. An optimized UCSO methyl ester yield of 92.00 % was obtained at a 1:10.80 molar ratio, 2.5 wt. % catalyst concentration, 80 minute reaction time, and 60 °C reaction temperature. The experimental yield was 92.10 %, as determined by the optimized yield based on these parameters. This shows that the response surface methodology is a successful strategy for increasing the yield. The regression model proved successful, as observed by the error values between the predicted and actual outcomes being less than 1 % UCSOME conversion. For this study, adequate precision was 8.9518. As a result, the model can be utilized to explore the design space. Each succeeding cycle of reuse produced 91.60 %, 85.50 %, 81.60 %, 78.60 %, 74.20 %, and 72.87 % of the biodiesel. The measurements for viscosity, density, and flash point of UCSO were 33-36 mm^2/s at 311 K, 911-916 kg/m^3 at 288 K, and 504-510 K, respectively. UCSO methyl ester (UCSOME) had a viscosity between 3.6 and 3.7 mm^2/s and a density between 875 and 880 at 311 K. While the flash points of the UCSOME are measured at 435–440 K as opposed to 504-510 K. The saponification value of cottonseed oil was 188.32 mg/g while that of biodiesel was 165.87 mg/g. Thus, biodiesel fatty acid methyl ester possesses a distinctive FTIR absorption of carbonyl (C=0) stretching vibrations near 1740-1744 cm^{-1} and C-O bending vibrations in the range of 1196 cm^{-1}.

---

* Corresponding author.; e-mail: abjimoh@abu.edu.ng.

https://doi.org/ 10.22034/CRL.2023.359632.1179

1.Introduction

The world is currently experiencing a worsening energy crisis as a result of the quick depletion of fossil fuels and the progressive rise in living standards. The globe is heavily dependent on dwindling non-renewable energy sources, including gasoline, diesel, and other fossil fuels. It is estimated that the present gasoline and diesel reserves will soon run out [1][2]. To address the escalating global energy dilemma, scientists from around the world have made a number of efforts to develop environmentally benign fuels. One such renewable fuel that is receiving more attention is biofuels, which have benefits including renewability, biodegradability, and environmental friendliness. Additionally, it significantly contributes to reducing both dependence on conventional fuels and global warming [3][4][5]. Biofuels are made from renewable energy sources like animal fat, used cooking oil, and vegetable oils (both edible and non-edible). Waste and Biomass Valorization, liquid biofuels (biodiesel, bioethanol), gaseous biofuels, and solid biofuels (wood, sewage) are the different categories of biofuels (methane, hydrogen). Conflicts between the production of food and the consumption of fuel result from the usage of vegetable oil for biodiesel, which demands land for production and increases food prices [6][7][8][9][10][11]. According to reports, feedstock accounted for between 70 % and 95 % of total production costs. Waste Cooking Oil (WCO) is one of the inexpensive and widely accessible raw materials used in the production of biodiesel. Not only can using WCO as fuel cut feedstock costs by 60 – 70 %, but it also prevents environmental contamination brought on by their disposal. Thermal cracking of vegetable oils, transesterification, microemulsions in diesel fuel, and direct usage or blending with diesel fuel are all methods used to produce biodiesel [12][13]. The process used to produce biodiesel that is most economical is transesterification. Fatty acid methyl esters (FAME) and glycerol are produced when triglycerides and methanol combine during the transesterification process in the presence of a catalyst (byproduct) [14][15][16]. The main categories of the catalysts used to produce biodiesel are homogeneous and heterogeneous catalysts. The quantity of free fatty acids (FFA) in the raw material affects the catalyst choice. When the raw material has a high FFA %, an acid catalyst was used; when the FFA content is less than 2 %, a base catalyst was utilized. At low temperatures and with a short reaction time, homogeneous catalysts yield high biodiesel conversion, but the separation of the biodiesel is challenging. Consequently, it produces soap, lowers catalytic effectiveness, and increases viscosity, all of which cause the development of gel [17][18]. Heterogeneous catalysts are non-corrosive, environmentally friendly, and simpler to separate from liquid byproducts despite the longer reaction time associated with the three-phase formation. Therefore, the goal of the current study is to produce a novel, economical, and environmentally friendly heterogeneous base catalyst. Activated oxides of magnesium and calcium, zeolites, hydrotalcite, γ-alumina, metal oxides supported on silica, and mixed oxides of TiO_2-MgO are a few examples of the heterogeneous catalysts that have been produced. Alkaline earth oxides are increasingly used among different heterogeneous catalysts because of their strong basicity and catalytic activity. However, the decomposition of organic elements in the dumped waste will result in hazardous odours if left untreated for an extended length of time. Thus, it may also have a negative impact on quality of life and health of the locals. It is crucial to determine whether these shells are appropriate for various applications in order to safeguard the environment in a secure and clean manner. The predominant component of these waste shells was calcium carbonate, which has received a lot of attention recently for the formation of a heterogeneous catalyst for the production of biodiesel. In the current study, waste materials for the transesterification of used cottonseed oil included eggshell and coconut husk waste. Several researchers have taken advantage of various waste shells, including eggshells [19][20] and clam shell [21][22]. *Tellina tenuis* shell [21] *Turbonilla striatula* shell [23], *Scylla Serrata* shell [24][25] *Anadara granosa* shell [25], *Pomacea sp.,* shell [26], Oyster shell [27], and obtuse horn shell [28] for the synthesis of CaO based catalyst. This waste shells CaO, possesses a moderate level of catalytic activity, hence is successfully employed as a heterogeneous catalyst for the synthesis of biodiesel. A variety of modification techniques have been used to develop CaO-based catalysts for high yield/conversion of biodiesel. [21] the calcination-hydration-dehydration approach improved the activity of the bivalve clam shell catalyst and raised the biodiesel yield to 94.25 %. [21] enriched the activity of CaO-based catalyst derived from *Tellina tenuis* shells by the wet-impregnation method and observed a high biodiesel conversion of 96.47 %. [29] using a 12:1 methanol to oil molar ratio and 5 wt. % catalysts at 65 °C, it was possible to produce a lithium doped CaO catalyst using the wet impregnation approach and convert 99.9 % of the resulting biodiesel.

[30] KOH was used to impregnate diatomite, producing a heterogeneous catalyst. At 30 % methanol to oil mass ratio, 5 % catalyst to oil mass ratio, 4 h reaction time, and 75 °C reaction temperature, the authors obtained 90 % biodiesel yields. [29] 99.9 % fatty acid ethyl ester (FAEE) yield was reported using a CaO-based catalyst that had been doped with molybdenum using the wet impregnation method at a 12:1 ethanol to oil molar ratio, a 5 % catalyst concentration, and a 65 °C reaction temperature. Since it requires a lot of experiments to determine the best locations, the conventional method of process optimization, known as one factor at a time (OFAT), is time-consuming and economically unviable. Response surface methodology (RSM), a modeling tool that uses a statistical approach to examine the interaction between process factors, was developed to address the aforementioned issues [31]. [24] they used an RSM-based CCD to optimize the transesterification of palm olein using a heterogeneous catalyst made from waste mud shells and observed the highest biodiesel purity at the optimum conditions of 0.5:1 methanol to oil mass ratio, 5 wt. % catalyst concentration, 65 °C reaction temperature, and 500 rpm stirring speed. [25] 98 % of the biodiesel was converted under ideal process conditions of 4.9 wt. % catalyst concentration, 0.55:1 methanol to oil mass ratio, and 3 h reaction time using CCD-based RSM to optimize the production of chicken fat-based biodiesel from catalysts derived from crab and cockle shells. Utilizing the calcined CaO catalyst made from eggshell and coconut husk waste as a heterogeneous base catalyst for the transesterification of UCSO is the primary goal of the current study. The calcined shells were subsequently activated by calcination at two different temperatures in order to enhance their catalytic activity. Waste coconut husk and eggshells were calcined to produce CaO, which exhibits superior catalytic activity, an alkaline characteristic, and a unique porous structure [20]. Therefore, in the current investigation, a highly active calcined CaO catalyst was used to transform spent cottonseed oil into biodiesel. RSM through Box-Behnken was employed to optimize the transesterification parameters, including the reaction temperature, catalyst concentration, reaction time, and methanol to oil molar ratio.

2.Experimental Methodology, Materials and Chemicals

10 liters of used cottonseed oil samples were purchased from a small restaurant in Funtua town, Katsina state, Nigeria. Thereafter, filtered to remove the inorganic scum. The FFA contents of the UCSO samples were determined using the colour indication titration method in accordance with ASTM D974 guidelines. It was discovered that the one-time UCSO had an acid value of 2.52 % and an FFA value of 1.26 %, indicating that no pretreatment step is required for the oil because its FFA value is less than 2.5 %. The transesterification process is limited to 3 % FFA because, above this level, the reaction process undergoes hydrolysis to produce soap and water, which lowers ester yield [32]. Methanol (99.8 % purity), isopropyl alcohol (99.9% Purity), and other chemicals were of analytical grade and were purchased from Sigma-Aldrich and British Drug House Ltd. (BDL), both in the UK.

2.1.Catalyst Preparation

The eggshell and coconut husk wastes were thoroughly rinsed with tap water and then cleansed twice with distilled water to eliminate any unwanted material that had adhered to their surface. The shell was then dried in a hot air oven set at 100 °C for 24 hours. The powder is sieved after it has been ground. The size of the eggshell powder and the coconut husk powder were both set at 250 μm. Thereafter calcined separately for 4 hours at 800 °C in a muffle furnace with static air at a heating rate of 2.5 °C/min. All calcined samples were kept in a closed desiccator before use to avoid reactions with carbon dioxide (CO_2) and humidity [33]. The transesterification procedure used catalyst, spent cottonseed oil, and methanol. Before the aforementioned procedures, 1 g of solid calcined coconut shell was added to 5 g of calcined ground eggshell. Calcined CaO-blend was then subsequent codename for this mixture [34].

2.2.Sample Characterizations

Under various conditions, the fatty acid content of the samples for the crude, purified, and synthesized biodiesel Used Cottonseed Oil Methyl ester (UCSOME) was evaluated using gas chromatography-mass spectrometry. Overall characteristics of these samples were examined, which include; acid number, viscosity, density, and flash point. Fourier Transform Infrared (FTIR) spectroscopy was used to identify the presence of a functional group in the calcined CaO-blend (Perkin Elmer 1000 spectrometer; Perkin Elmer, Waltham, MA, USA), and a contrast between the functional group present in CaO that is produced commercially was drawn. A scanning electron microscope (SEM) was used to examine the surface morphology of the synthesized catalyst. EDS analysis (JEOLJSM-600F) was also used to determine the elements present in the synthesized catalyst, and X-ray diffraction (XRD) analysis (XRD Rigacu MiniFlex 300) was employed to confirm that the catalyst produced is calcium oxide (CaO) [33].

2.3.Fuel Property Analysis

A number of physical and chemical characteristics of the biodiesel are measured before it was used as fuel to assess its fuel quality. Many of parameters of the biodiesel were assessed using IS-1448 (Methods of Test for Petroleum and Its Products). To determine the moisture content, a Karl Fischer moisture titration was employed. The values of saponification and iodine were determined using titration. Pensky-Martens equipment were employed in measuring the flash point and fire point. A pycnometer was used to determine specific gravity. The cetane number is calculated using Eq. (1) [35].

$$\text{Cetane number} = 46.3 + 5458/\text{Saponification value} - 0.225 \times \text{Iodine value}$$

2.4.GCMS Analysis

The relative percentages of certain Fatty Acid Methyl Esters (FAME) in used cottonseed oil and biodiesel were assessed using gas chromatography. The Trace GC Ultra gas chromatograph from Thermo Scientific features an EI (electron impact) detector, a 30 m long, 0.25 mm ID, and 0.25 film thickness Agilent TR-Wax MS column. Helium gas with a purity of 99.99 % and a flow rate of 1 cm^3/min serves as the carrier gas. The split ratio stays the same at 1:20. After the sample has been filtered using a syringe filter, 1 L of it was injected (Make: Millex; Model: GV; Pore Size: 0.22 m^{-1}). The temperature of the oven was kept at 70 °C for a hold-up period of 2 minutes. The temperature of the oven was then increased to 100 °C at a rate of 10 °C per minute and held there for two minutes. The temperature of the oven was then raised to 250 °C and held there for 5 minutes at the same pace of heating. The set-point temperature of the oven was maintained at 250 °C. For data analysis, Xcalibur software is employed.

3.Design of Experiments

In the current study, a four-level Box-Behnken Design (BBD) in response surface methodology (RSM) was used to increase the percentage yield of UCSOME in response to the transesterification reaction of UCSO samples. A: Molar ratio, B: Reaction temperature, C: Catalyst concentration, and D: Reaction Duration were the independent variables for the experiment. The significance of each component, interaction, and quadratic term in the optimization process was evaluated using statistical analysis tools [Design Expert program version 11.0.0 Stat Easy, Minneapolis, USA]. Each component was altered at three different levels, -1, 0, and +1, which stand for low, medium, and high values. The organizational structure of the factorial design is shown in Table 1.0. A total of 27 experiments were employed in this study to evaluate the effects of the four main independent parameters on the percentage yield of UCSOME production. A non-linear regression model was used to fit the second-order polynomial (Eq. (1)) identifying the pertinent model terms in relation to the experimental data. The obtained experimental data was first fitted to a variety of models, including the linear, 2FI, quadratic, and cubic models using the program in order to determine the statistically significant model, as shown in Table 3. The quadratic response model can be represented by Eq. (1) when all the linear terms, square terms, and linear by linear interaction items are considered:

$$\text{Yield} = \beta_o \pm \sum_{i-1}^{n} \beta_i X_i \pm \beta_{ii} X_i^2 \pm \sum_{i=1}^{n=1} \sum_{i=0}^{n} \beta_{ij} X_i X_j \quad (1)$$

Where; Yield represents an objective to optimize the response as a percentage of used cottonseed oil methyl ester yield, β_o = constant-coefficient, β_i = regression coefficient of the linear terms, β_{ii} = regression coefficient of the quadratic terms, β_{ij} = regression coefficient of the interaction terms, and X_i and X_j are independent variables [36].

Table 1: Variables in the Process for the Box Behnken Design

Factors	Parameters	Units	Low	Medium	High
A	Molar ratio	mol/mol	1:10	1:10.4	1:10.8
B	Reaction temperature	°C	50	55	60
C	Reaction time	min	50	80	110
D	Catalyst Concentration	wt.%	1.0	2.5	4.0

For the transesterification reaction; methanol to oil molar ratio in mol/mol, reaction temperature in °C, CaO concentration in units of wt. %, and reaction duration in min were all subjected to an optimization design consisting of 27 runs. A 500 cm^3 three-necked round-bottomed flask with a reflux condenser was used to conduct the transesterification reaction. A mechanical stirrer running at an appropriate rotation rate per minute (rpm) was used to stir the mixture. Each experiment was conducted using a sample of 50 g UCSO reactants with the addition of a heterogeneous alkali-calcined CaO-blend catalyst produced from a waste mixture of eggshell and coconut husk. The Gallenhamp magnetic stirrer hot plate was employed to warm the reaction flask. Following the reaction period, the mixture was placed into a 75 cm^3 sample tube and centrifuged for 15 minutes. The upper layer was then transferred into a separating funnel to separate the ester and traces of glycerol layer. Glycerol, extra methanol, and other compounds were removed from the lower layer. The top layer of methyl ester was scraped off and then washed with phosphoric acid (0.1 wt. %) and distilled water to remove any remnants of methanol, glycerol, and catalyst. The methyl ester was washed repeatedly until the final product solution had a pH of 7. Finally, to remove the moisture content, the product was heated to 100 °C [37][38].

Table 2: BoxBehnken Design (BBD) Matrix with Experimental Data and Response

Runs	**Factor 1 A:Methanol/Oil ratio (wt%)**	**Factor 2 B: Reaction Temperature (°C)**	**Factor 3 C: Reaction Time (min)**	**Factor 4 D: Catalyst Conc. (wt%)**	**Response 1 UCSOME yield (%)**
1	10.4	55	110	4.00	82.60
2	10.4	55	50	1.00	80.40
3	10	60	80	2.50	71.20
4	10.4	60	80	1.00	82.20
5	10.4	60	50	2.50	82.50
6	10.4	50	80	4.00	85.40
7	10	50	80	2.50	70.40
8	10	55	50	2.50	73.40
9	10	55	110	2.50	76.00
10	10.4	55	80	2.50	83.20
11	10.4	55	80	2.50	84.20
12	10.4	55	50	4.00	85.20
13	10.4	50	50	2.50	81.20
14	10.8	55	50	2.50	90.20
15	10.8	55	110	2.50	90.50
16	10.8	60	80	2.50	92.00
17	10.4	50	80	1.00	80.20
18	10.4	55	80	2.50	82.20
19	10.4	55	110	1.00	81.20
20	10.4	60	110	2.50	83.20
21	10	55	80	4.00	74.60
22	10	55	80	1.00	72.20
23	10.8	55	80	4.00	82.60
24	10.8	50	80	2.50	80.20
25	10.8	55	80	1.00	80.20
26	10.4	50	110	2.50	84.40
27	10.4	60	80	4.00	85.10

Eq. (2) is used to determine biodiesel yield;

$$\text{Biodiesel Yield } (\%) = \frac{(\text{mass of biodiesel produced in gram})}{(\text{ mass in grams of raw oil taken for reaction})} \times 100 \qquad (2)$$

3.1.Discussion of the Findings

3.1.1.BBD model analysis

A total of 27 experiments (runs) were produced using BBD (Table 1). A: molar ratio, B: reaction temperature, C: catalyst concentration, and D: reaction duration were taken into consideration as process parameters for the four factors under examination, as well as their individual and combined effects on the UCSOME yield (as a response) i.e. the independent factors were investigated using the BBD approach. The mathematical formulation of the link between the response and the process components was produced using a quadratic polynomial model. The results of the ANOVA tests were assessed for significance of the regression model for the response, and Table 3 displays the findings. Model terms Prob>F<0.0500 values show that certain conditions make certain factors significant. Response (%UCSOME yield) important model term is A. It was discovered that the other element previously indicated has a greater impact on the percentage of UCSOME production efficiency than D-reaction time, AC, AB, B, C, AD, BC, CD, BD, A^2, B^2, C^2, and D^2. The empirical relationships between tested factor and response are presented according to the following Eq. (3):

$$\text{UCSOME yield} = +84.42 + 0.0812\,A + 0.0143\,B + 0.0053\,C + 0.0196\,D + 0.0315\,AB - 0.0079AC - 0.0008AD - 0.0076\,BC - 0.0070\,BD - 0.0102CD - 0.0479\,A^2 - 0.0069\,B^2 + 0.0138\,C^2 - 0.0144\,D^2 \qquad (3)$$

A positive sign in Eq. (3) denotes a synergistic effect of the factor, whereas a negative sign denotes an antagonistic effect of the factor [39]. As shown in Fig. 6, the results of an ANOVA analysis for response factors show that the R-squared (determination coefficient) value is very high 0.8793, indicating a strong connection between the actual and projected values (predicted vs actual plot).

3.1.2.Analysis of variance (ANOVA)

The initial second-order quadratic model that was constructed using BBD (shown in Equation 3) and the most important variables in converting UCSO to biodiesel are evaluated by the ANOVA analysis of the BBD, which is also displayed in Table 3. Any obtained result must first undergo a successful validation before being plotted. The parameters, particularly the molar ratio (A), were significant because the p-value of the model was less than 0.05. The regression analysis indicates that a model is significant if the p-value is less than 0.05. Regression analysis shows that the UCSOME yield was significantly impacted by just one linear variable [40][41]. However, the F-value from the ANOVA analysis, which was found to be 6.25 for the model and 63.25 for the molar ratio (A), governs how well the yield response performs. The molar ratio high F-value indicates that it has a greater impact on the experimental variables that affect the conversion of UCSO to biodiesel (UCSOME). It is also clear from Table 3 that the lack of fit, which is used to assess the applicability of the model, was negligible with a p-value of 0.0926, indicating that there was less discrepancy between experimental data and findings predicted by the studies of BBD.

Table 3: ANOVA for the Quadratic Model Regression

Analysis of Variance for Values

Source	DF	SESQSS	ADJ SS	ADJ MS	F	p value prob>F
Regression	14	0.1093	0.1093	0.0078	6.25	0.0015
Linear	20	0.0376	0.0376	0.0019	13	0.0737
Square	4	0.0147	0.0147	0.7385	10.19	0.0926
Interaction	14	0.0325	0.0325	0.0023	16.08	0.0601
Residual	12	0.015	0.015	0.0013		
Lack of Fit	10	0.0147	0.0147	0.0015	10.19	0.0926
Pure Error	2	0.0003	0.0003	0.0001		
Cor Total	26	0.1244				

Term Coefficient

Source	Sum of Square	Df	Mean Square	F-value	p-value

Model	0.1093	14	0.0078	6.25	0.0015	Significant
A-MOLAR RATIO	0.0791	1	0.0791	63.26	3.99E-06	
B-REACTION TEMPERATURE	0.0024	1	0.0024	1.95	0.1874	
C-REACTION TIME	0.0003	1	0.003	0.2742	0.0794	
D-CATALYST CONCENTRATION	0.0046	1	0.0046	3.67	0.1002	
AB	0.004	1	0.004	3.17	0.1002	
AC	0.0002	1	0.0002	0.1982	0.6641	
AD	0.0002	1	0.000002583	0.0021	0.9645	
BC	0.0002	1	0.0002	0.1824	0.6769	
BD	0.0002	1	0.0002	0.1584	0.6976	
CD	0.0004	1	0.0004	0.3343	0.5738	
A^2	0.0122	1	0.0122	9.77	0.0088	
B^2	0.0003	1	0.0003	0.2058	0.6582	
C^2	0.001	1	0.001	0.8145	0.3846	
D^2	0.0011	1	0.0011	0.882	0.3662	

3.1.3.Characterization of Catalyst

The fourier transform infrared spectra of the samples were recorded using a Perkin Elmer 1000 spectrometer (Perkin Elmer, Waltham, MA, USA) in the transmittance mode with the KBr disk technique, with a spectral range of 4000-400 cm^{-1} and a resolution of 4 cm^{-1}. Figure 10 depicts the FTIR spectrum of the calcined CaO-blend in the range of 450-4000 cm^{-1}. The 0-H stretching vibrations of $Ca(OH)_2$, which are as a result of the moisture absorption from an environment on the surface of the pellets, is attributed to the occurrence of the spectra bands at 3638.99 cm^{-1} [42]. While the peak between 1406.21 cm^{-1} and 1430.33 cm^{-1} is the result of the Ca-O stretching bending vibration. Due to the $CaCO_3$ sample concentration, very small vibrations were detected at 2509.36 cm^{-1} [43]. Similar fluctuations were observed in bands at 1420, 1085, and 577 cm^{-1}, which is the result of the conversion of carbonate to CaO [44]. The band at 1406.21, 873.07, and 712.28 cm^{-1} (for calcined CaO-blend) in the spectra, corresponds to the stretching vibration of the CO_3^{2-} group, is attributed to the chemisorption of gaseous CO_2 from the atmosphere over the surface of the catalyst [45]. The presence of the stretching vibration mode of the Ca-O bond at 528 cm^{-1}, in addition, gave strong support for the production of Ca oxides during the calcination of the eggshell and coconut husk waste blend. Moreover, the absence of a peak for the $CaCO_3$ component in the FTIR spectra is an indication that all of the $CaCO_3$ components present in the eggshell and coconut shell blend were transformed into CaO. Hence, the calcined CaO-blend, has the same potential as commercial CaO to act as a heterogeneous catalyst in the production of biodiesel. The calcined CaO that was produced was further characterized using XRD Rigacu MiniFlex 300 operating in the reflection mode with copper radiation of wavelength (λ=1.54059Å) at 40 kV and 30 mA. The data was taken for the 2θ range of 5° to 80°. Similar to this, the XRD result obtained was matched with the JCPDS card number 37-1497 peaks corresponding to calcined CaO at 2θ = 19°, 35°, 49°, and 63° in Fig. 8, which shows successful calcination [46]. Using the Debye-Scherer equation, the average crystallite size of the calcined particles was calculated [47] and was found to be 111.30 nm (equation 3);

$$d = K\lambda/\beta \cos \theta \tag{3}$$

Where; β = full-width at half-maximum (in radian) and θ = is the position of the maximum of the diffraction peak. K is defined as the so-called shape factor, which usually has a value of about 0.9. λ = the X-ray wavelength (1.5406 Å for Cu Kα).

The result shows that calcined CaO has a face-centered cubic phase as its structure. It was confirmed by the XRD pattern that CaO with cubic phase is formed; these results were comparable to those obtained by [48][49][50][51]. The results obtained were also comparable to those of [52] [53]. The exposure of the calcined catalyst to atmospheric air prior to analysis can be attributed to the minor hexagonal-shaped $Ca(OH)_2$ peaks that were observed at 29°, 30°, 48°, 65°, and 72°. Peaks at 29.36° and 44° show the presence of $CaCO_3$ species with a rhombohedral structure [28]. In addition, the catalyst shape and elemental contents were assessed utilizing SEM with a ZEISS EVO LS10 operating at 20 kV. Furthermore, calcined CaO exhibits a maximum particle size reduction and a higher surface area which are two key characteristics of heterogeneous catalysts. The SEM image of the calcined CaO clearly depicts uniform particle morphologies with clusters of well-developed cubic crystals and a distinct reduction in particle sizes, indicating larger surface area which is beneficial for the transesterification reaction [54] as shown in fig. 9b. The purity of the calcined CaO is shown by the two peaks of Ca (71.5 %) and O (28.5 %) in the EDX spectra, which were recorded as shown in figure 9b.

3.2.Operating Parameter Effects on UCSO Methyl Ester Yield

3.2.1.Methanol to Oil Ratio and Catalyst Concentration Interaction

The effects of the methanol to oil molar ratio (A) and catalyst concentration (B) are shown in Figures 2a and b. While the catalyst concentration was adjusted from 1 to 4 wt. % and the methanol to oil molar ratio from 10:1 to 10.8:1, the reaction duration and temperature were kept constant at 80 mins and 55 °C, respectively. The 3D response surface plots are shown in Figure 2a, whereas the 2D contour plot is shown in Figure 2b. It was shown from the plots that, in comparison to other reaction parameters, the methanol to oil molar ratio (minimum p-value) has a significant impact on the conversion of biodiesel. The biodiesel conversion is dramatically increased by increasing the methanol to oil molar ratio. Due to the ineffective mixing of the reactants, a greater catalyst concentration with a low methanol to oil molar ratio drastically lowers biodiesel conversion, and additional methanol is required to shift the equilibrium in order to maximize the biodiesel conversion [31][43]. However, increasing the methanol to oil ratio over the optimum level will make it more difficult to separate glycerol from biodiesel because glycerol becomes more soluble in the biodiesel phase [55]. Maximum biodiesel conversion (92 %) was obtained at a methanol to oil molar ratio of 10.8:1, which is in accordance with the findings of [43] the scientists stated that 12:1 was the optimum methanol to oil molar ratio for the production of biodiesel utilizing waste cooking oil and CaO catalysts synthesized from ostrich and chicken eggshells.

3.2.2.Relationship between Catalyst Concentration and Reaction Time

At a constant methanol to oil molar ratio of 10.4:1, Figures 3a and b show the interaction between reaction time and catalyst concentration on biodiesel conversion. The biodiesel conversion was obtained at 83.50 % with a shorter reaction time and minimal catalyst concentration, and it slightly increased with an increase in catalyst concentration. As the catalyst concentration increases, more basic sites become available, which improves the conversion of biodiesel. Because of the poor mixing caused by the rise in reaction mixture viscosity, increasing the catalyst concentration above the optimum level will limit the amount of biodiesel that is converted [56]. To some extent, however, extending the reaction time considerably improves the conversion of biodiesel, and with additional increases, esters will hydrolyze, resulting in the synthesis of soap [57]. It is clear from the plots that the maximum biodiesel conversion occurs at 80 minutes.

3.2.3.Methanol to Oil Molar Ratio and Reaction Time Interaction

At a constant catalyst concentration of 2.5 wt. %, Figures 4a and b show the 3D response surface plot and 2D contour plot for the interactions of methanol to oil molar ratio (A) and reaction time (C) on the biodiesel conversion. Enhancing biodiesel conversion involves extending the reaction time up to 80 minutes while maintaining a low methanol to oil molar ratio. A decrease in biodiesel conversion was noticed as the reaction time was increased above 80 minutes. Due to the occurrence of the reverse reaction, which results in the synthesis of soap, this decrease in biodiesel conversion indicates the loss of esters [58]. [43] observed identical results on a catalyst produced from used ostrich and chicken eggshells, and they discovered that biodiesel conversion decreased with longer reaction times. A longer reaction period of 80 minutes and a higher methanol to oil molar ratio led to a higher biodiesel conversion (>80 %) (beyond 10.4:1). The methanol to oil molar ratio was clearly the most important factor for optimizing biodiesel conversion, as shown by the ANOVA table, where it has a very low p-value (<0.0001) and a high F value (63.26).

3.2.4.Temperature and Methanol to Oil Ratio Interaction

Figures 5a and b show the three-dimensional response surfaces plot for the % UCSOME yield between molar ratio and reaction temperature at 80 min of reaction duration and 2.5 wt. % catalyst concentrations. 83.8 % was the UCSOME yield that was achieved as optimum. The amount of biodiesel produced is significantly impacted by the increase in molar ratio and reaction temperature. Thus, the optimum biodiesel yield is acquired at a high value of molar ratio and reaction temperature i.e., 10.3 molar ratio and 54 °C temperature. But too much methanol increases the solubility glycerol and prevents it from being separated from the methyl ester [59].

3.2.5. Optimized Reaction Conditions

The Design-Expert software 11.0.0 numerical optimization method was used to find the optimum conditions for maximizing biodiesel conversion. By producing an overlay plot, the optimization procedure was carried out to determine the values of the affected variables that would produce the best biodiesel yield while taking into consideration all input parameters (Figure 1). In order to determine the best location for each variable, the data on the overlay plot were computed using the derived model equation. The restrictions stated in Table 4 were defined to produce the optimal region:

(1) The molar ratio was established to be between 10:1 and 10.8:1. However, due to the reversibility of the reaction, too much methanol is required to move the reaction to the product side.

(2) The reaction temperature was fixed between 50 and 60 °C. This is due to methanol boiling point. Methanol will evaporate if the temperature range is increased above what is necessary for this experiment.

(3) Reaction time is a key element in industry. The goal was to produce as much biodiesel as possible in a short amount of time. Therefore, for the optimization, a reaction time range of 50 to 110 minutes was chosen. The process was optimized based on the established boundaries.

(4) To prevent side reactions with the reactants that could result in soap production, the catalyst concentration goal was fixed at 3.0 wt. %. The process was optimized based on the established boundaries.

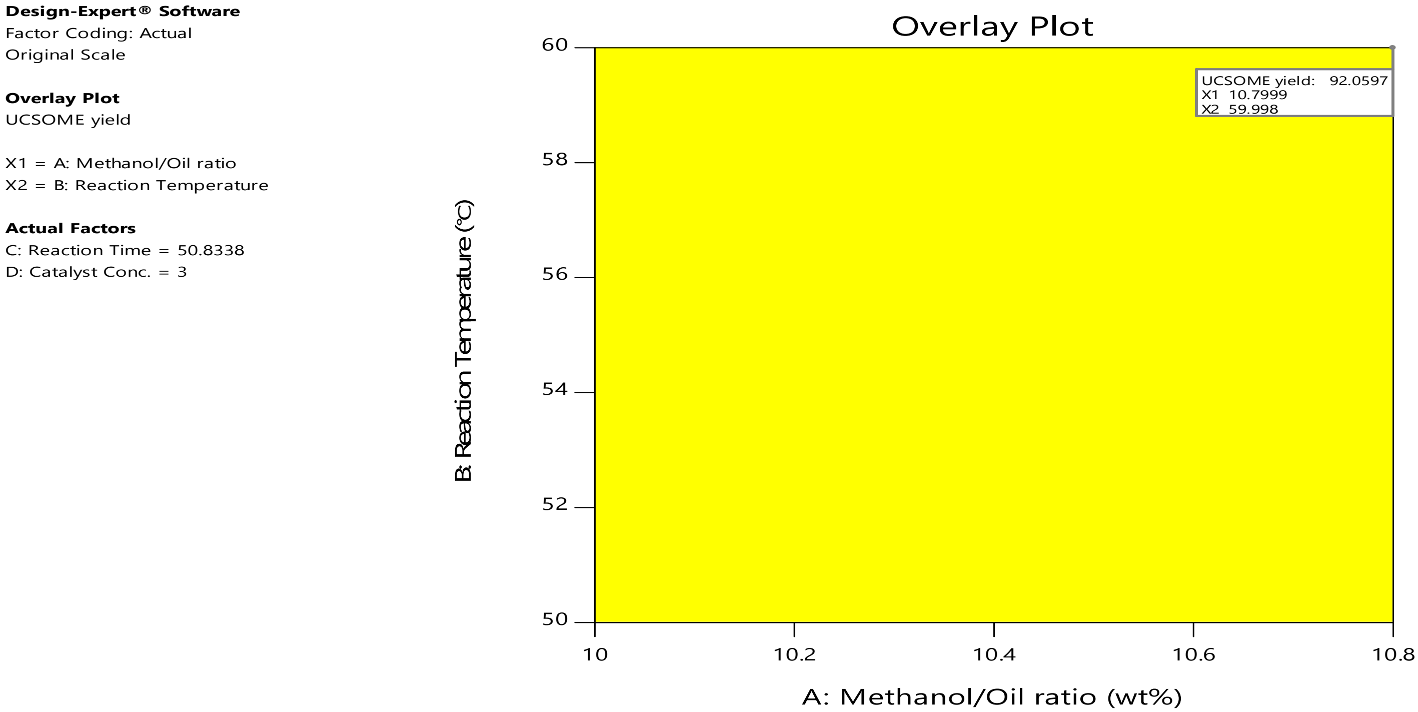

Figure 1: Overlay plot for the prediction of biodiesel production using calcined CaO blend heterogeneous catalyst

The average observed value of 92.00 % and the expected conversion value of 92.10 % were nearly identical. As a result, there was a respectable level of agreement between the experimentally obtained value and the projected values. The regression model proved successful, as observed by the error values between the predicted and actual outcomes being less than 1 % UCSOME conversion. The R-squared in Table 7 was examined in order to confirm the model appropriateness. A high R^2 value is preferred, and it is critical that adjusted R^2 and predicted R^2 coincide to a reasonable degree [60].

Table 4: Numerical Optimization Results and Constraints for the Factors/Response

Parameter	Goal	Experimental Region	
		Lower	Upper

Molar ratio (mol/mol)	In range	10:1	10.8
Reaction temperature (°C)	In range	50	60
Reaction time (min)	In range	50	110
Catalyst concentration (wt%)	Target	-	3.0
UCSOME YIELD (%)	**maximize**		

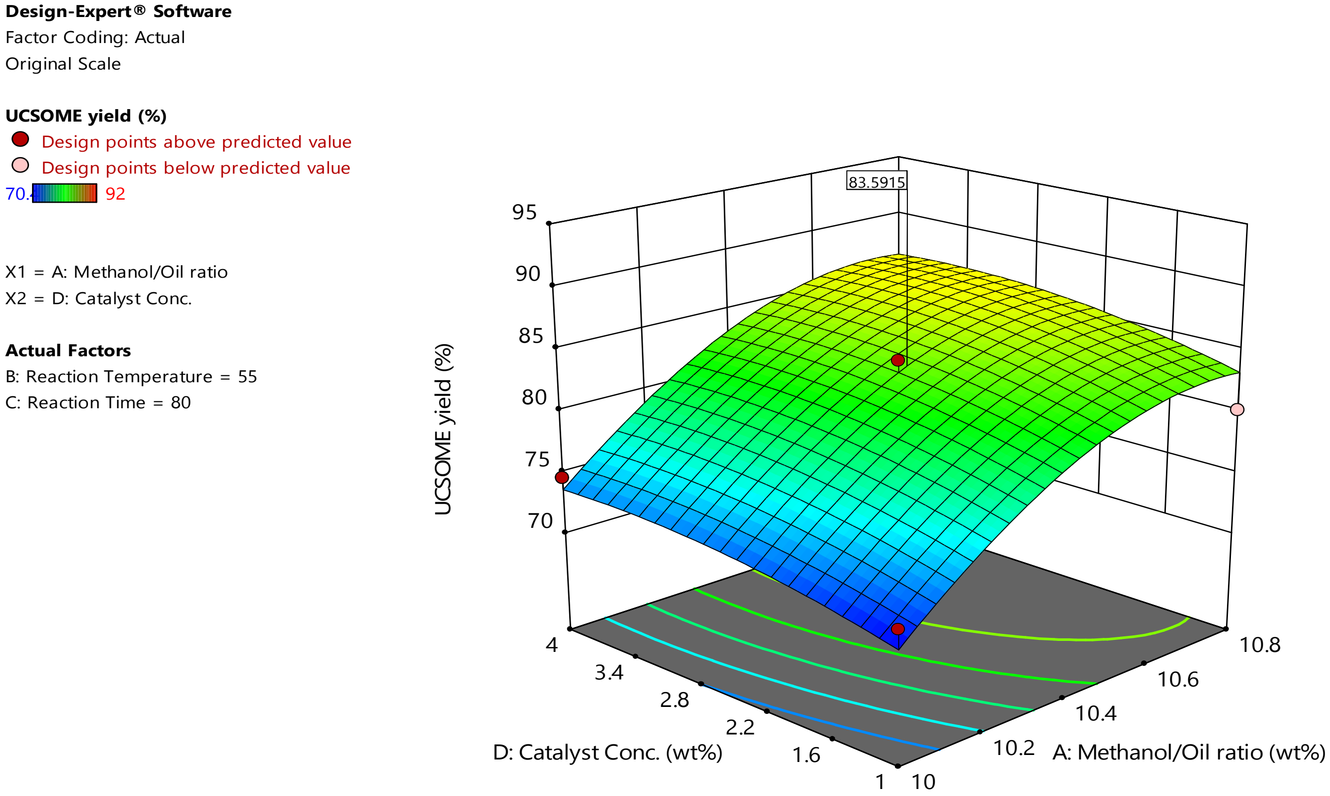

Figure 2a: Response surface plot between methanol/oil ratio and catalyst concentration at reaction temperature 55°C and 80 min reaction time

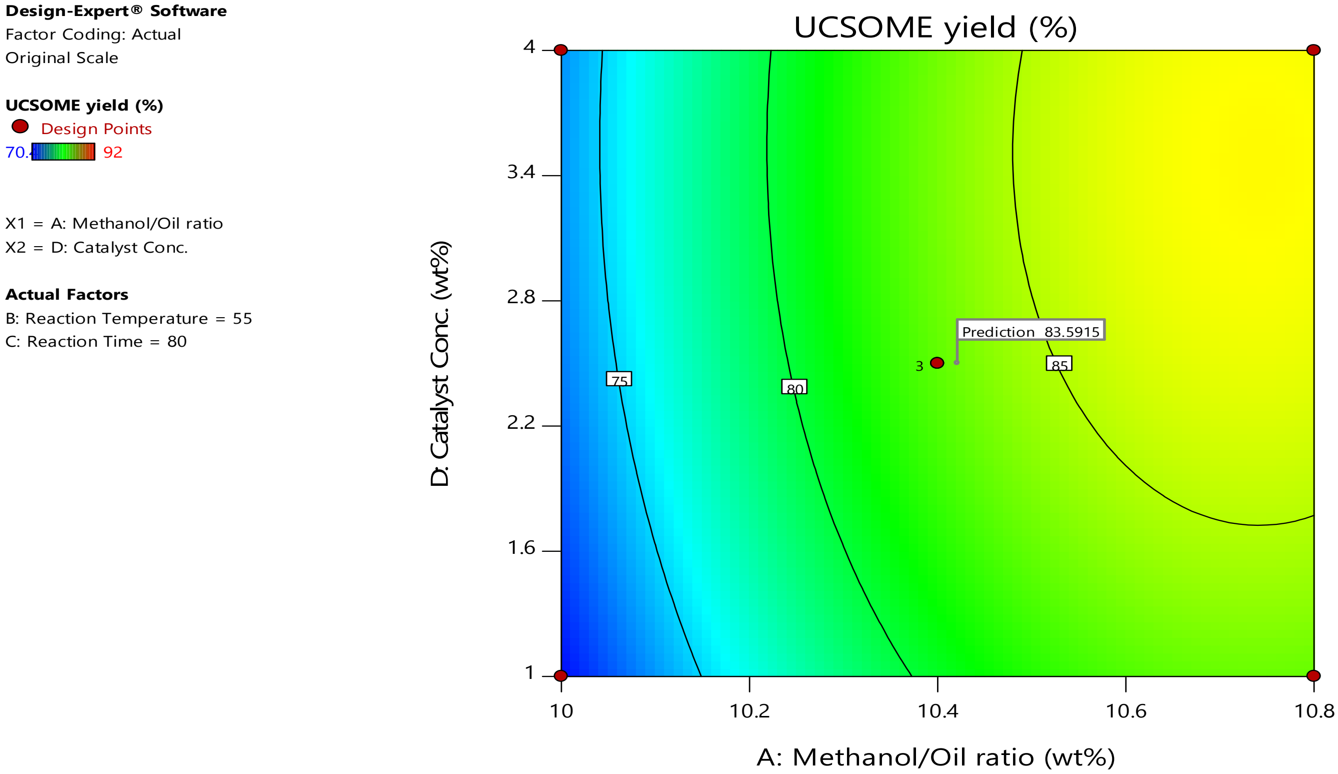

Figure 2b: Contour surface plot between methanol/oil ratio and catalyst concentration at reaction temperature 55°C and 80 min reaction time

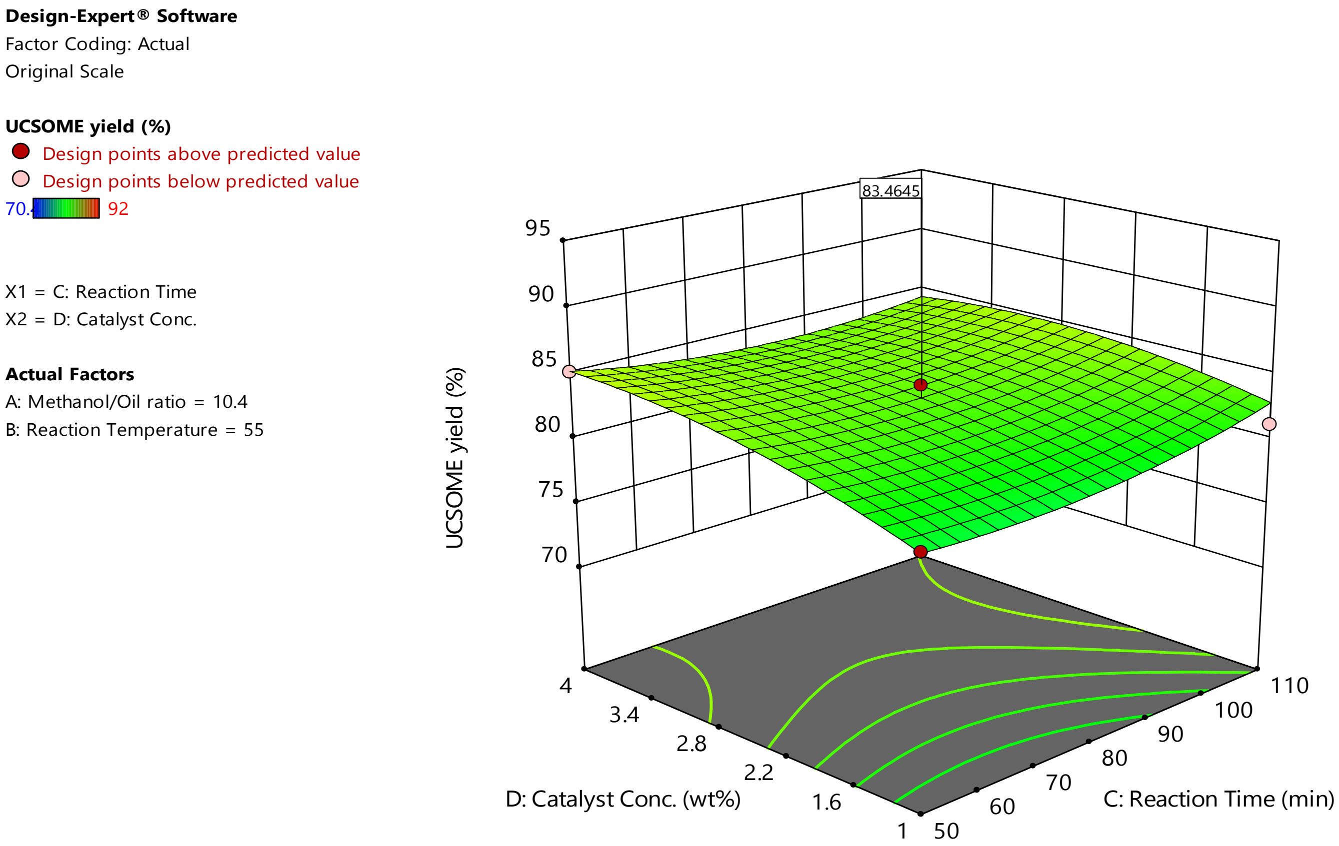

Figure 3a: Response surface plot between catalyst concentration and reaction time at methanol/oil ratio 10.4 and 55°C reaction temperature

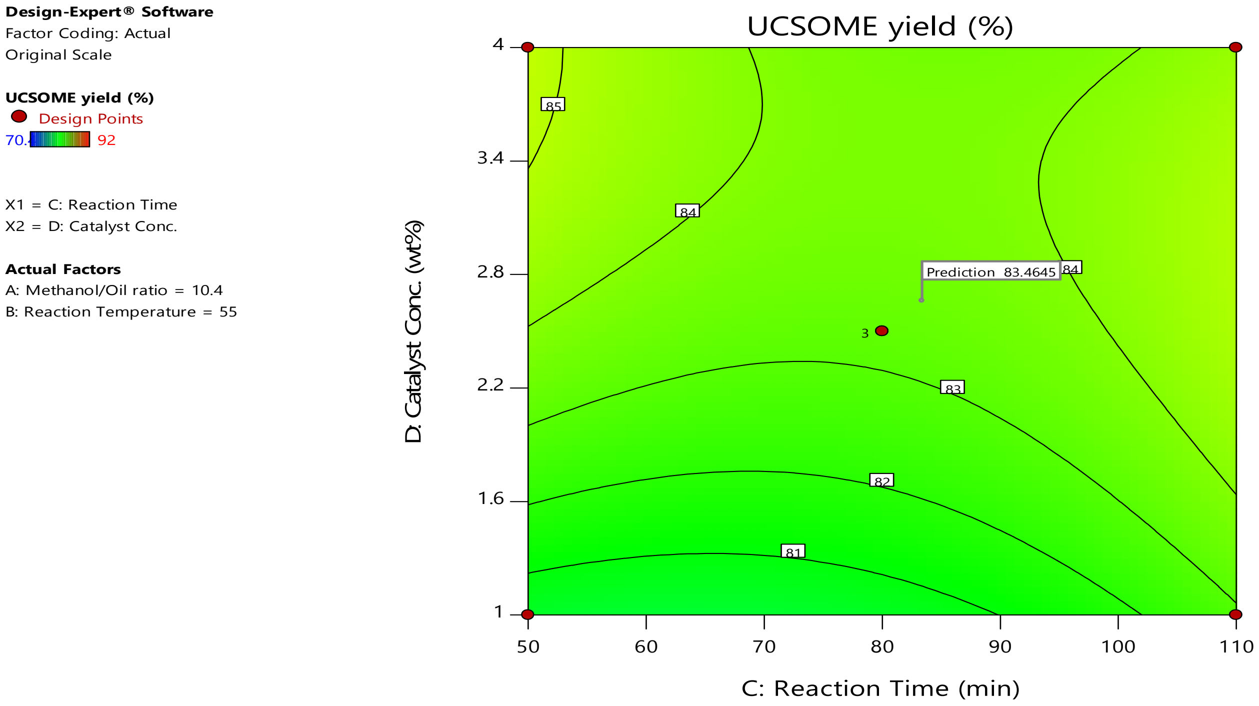

Figure 3b: Contour surface plot between catalyst concentration and reaction time at methanol/oil ratio 10.4 and 55 °C reaction temperature

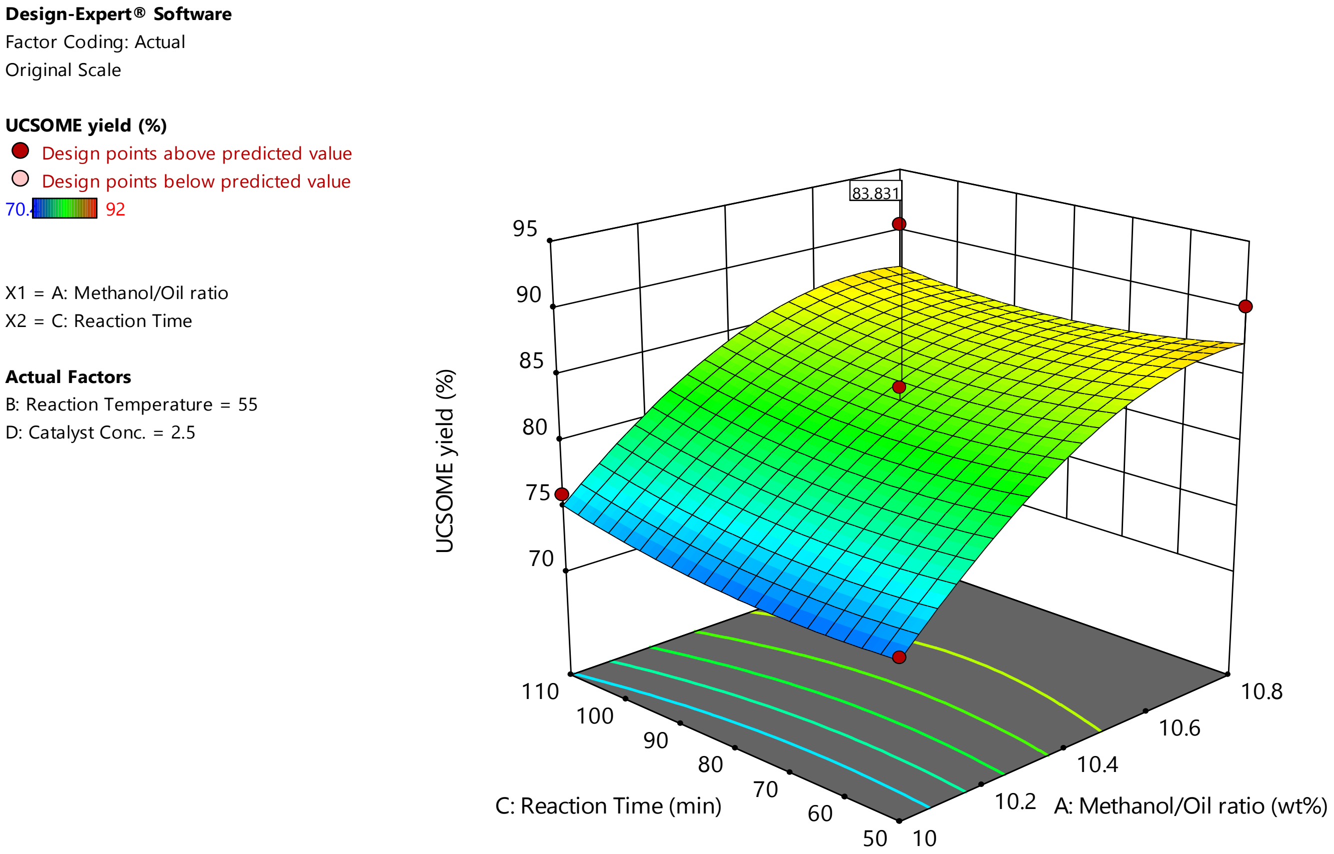

Figure 4a: Response surface plot between methanol/oil ratio and reaction time at reaction temperature 55 °C and 2.5 g catalyst concentration

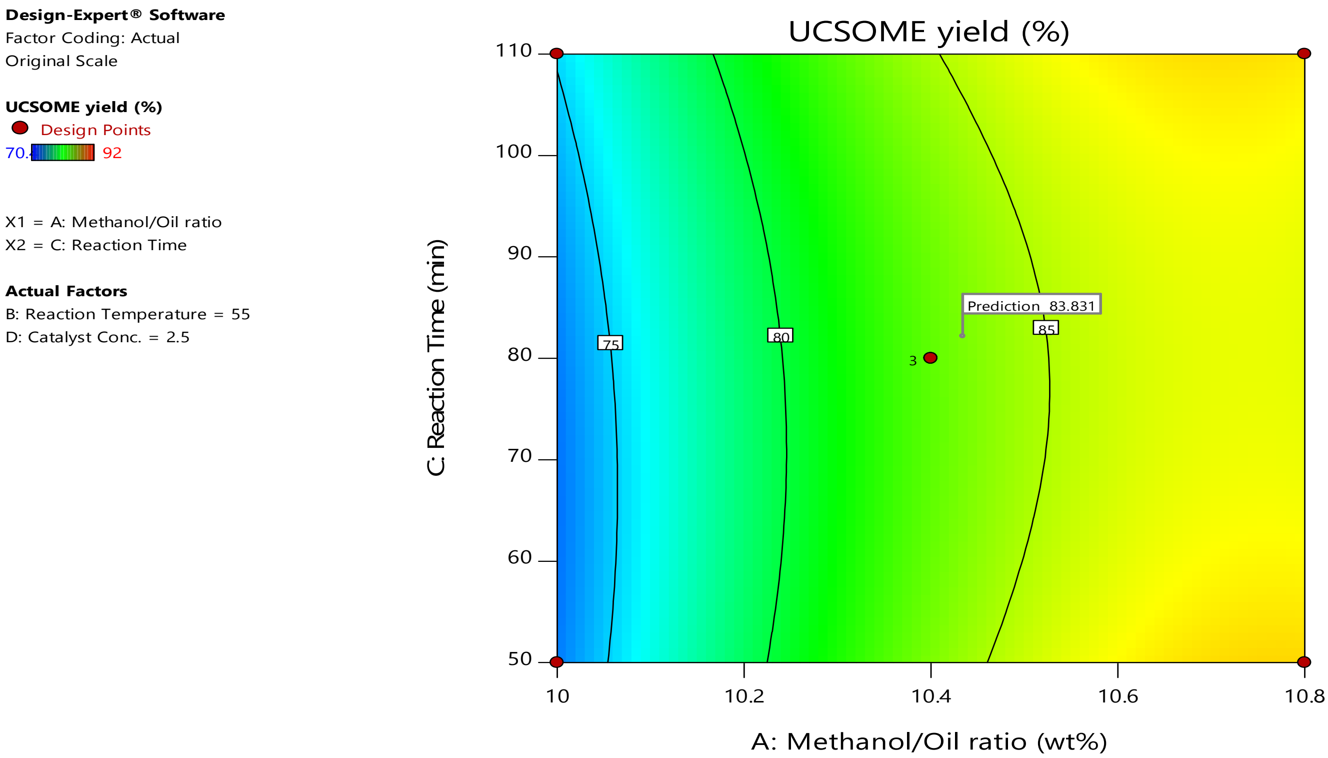

Figure 4b: Contour plot between methanol/oil ratio and at reaction temperature 55°C and 2.5 g catalyst concentration

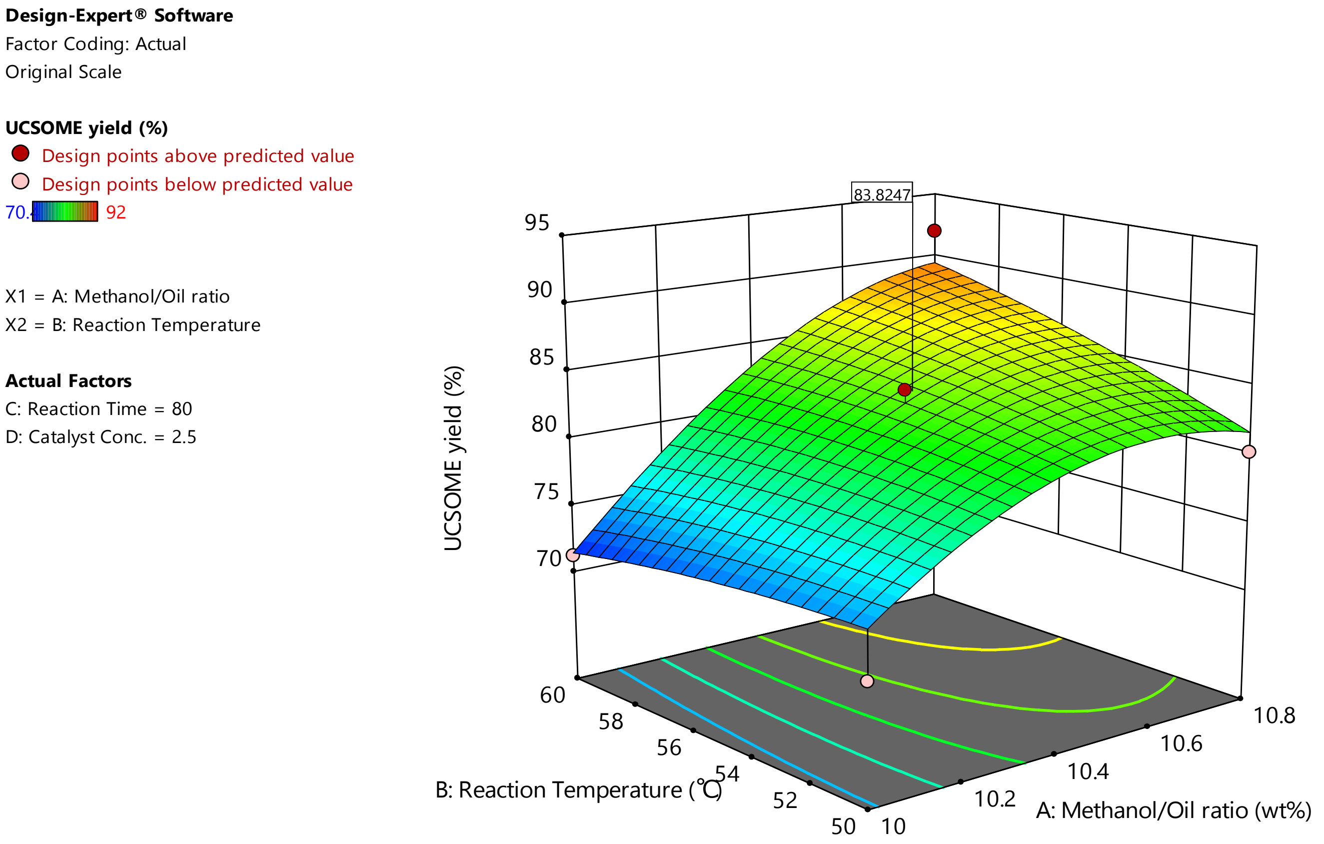

Figure 5a: Response surface plot between methanol/oil ratio and reaction temperature at reaction time 80 min and 2.5 g catalyst concentration

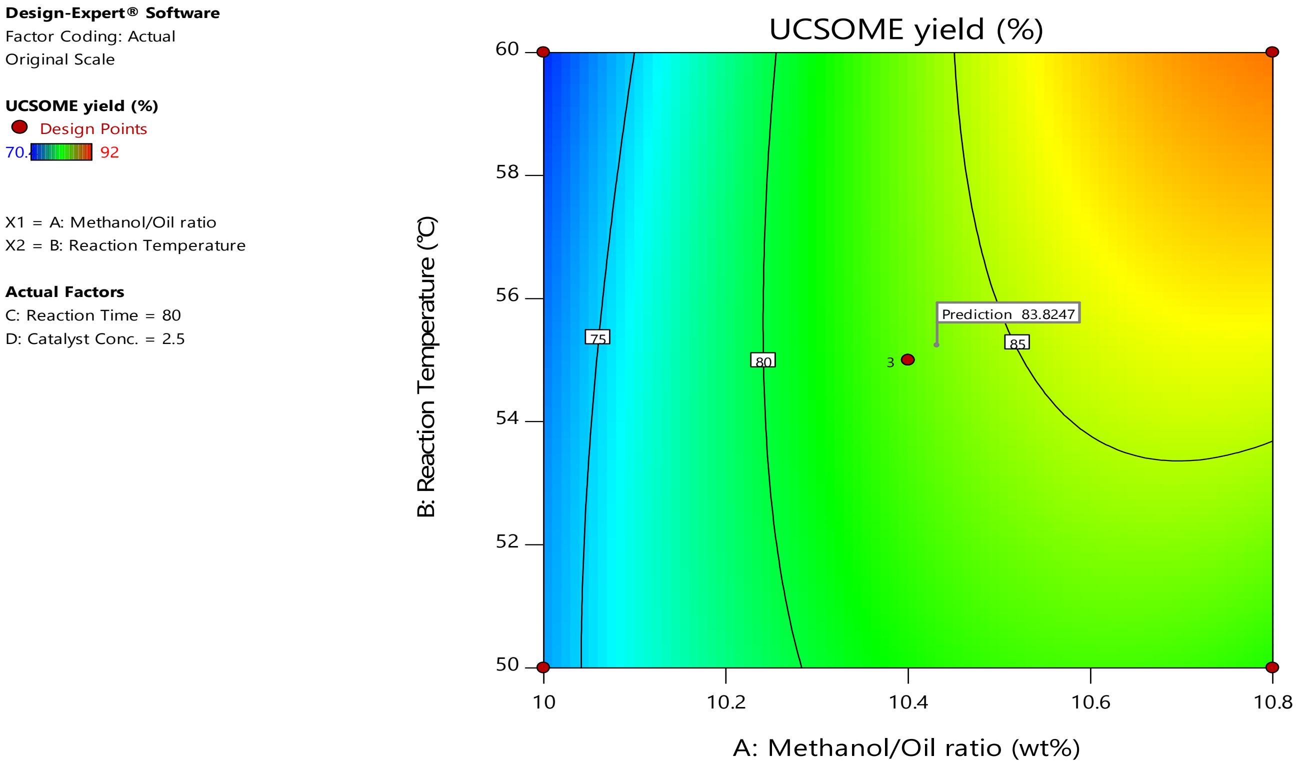

Figure 5b: Contour plot between methanol/oil ratio and reaction temperature at reaction time 80 min and 2.5 g catalyst concentration

Table 5: The Result of Optimum Values

Parameter	Units	Code	BBD Theoretical value
UCSOME Yield	**(%)**	**Y**	92.10
Molar ratio	**(mol/mol)**	**A**	10.80:1
Reaction temperature	**(°C)**	**B**	59.00
Reaction time	**(min)**	**C**	69.40
Catalyst concentration	**(g/L)**	**D**	3.0

Table 6: Verification of the Design Models

Parameter	Units	Code	BBD	
			Theoretical value	Experimental Value
UCSOME Yield	**(%)**	**Y**	92.10	92.00
Molar ratio	**(mol/mol)**	**A**	10.80:1	10.80:1
Reaction temperature	**(°C)**	**B**	59.00	60
Reaction time	**(min)**	**C**	69.40	80
Catalyst concentration	**(wt%)**	**D**	3.0	2.5

Table 7: The R-Squared Results

Std. Dev.	0.0354	**R²**	0.8793
Mean	74.38	**Adjusted R²**	0.7385
C.V. %	4.4	**Predicted R²**	0.3131
PRESS	0.0854	**Adeq Precision**	8.9518
-2 Log-Likelihood	-125.75	**BIC**	-76.31
		AICc	-52.11

Adequate precision (AP) is defined as a measure of the experimental signal-to-noise ratio [61]; an AP that exceeds 4 usually indicates that the model will give a reasonable performance in prediction. The "Adeq Precision" for this study was 8.9518. Therefore, the model was suitable to be used to navigate the design space.

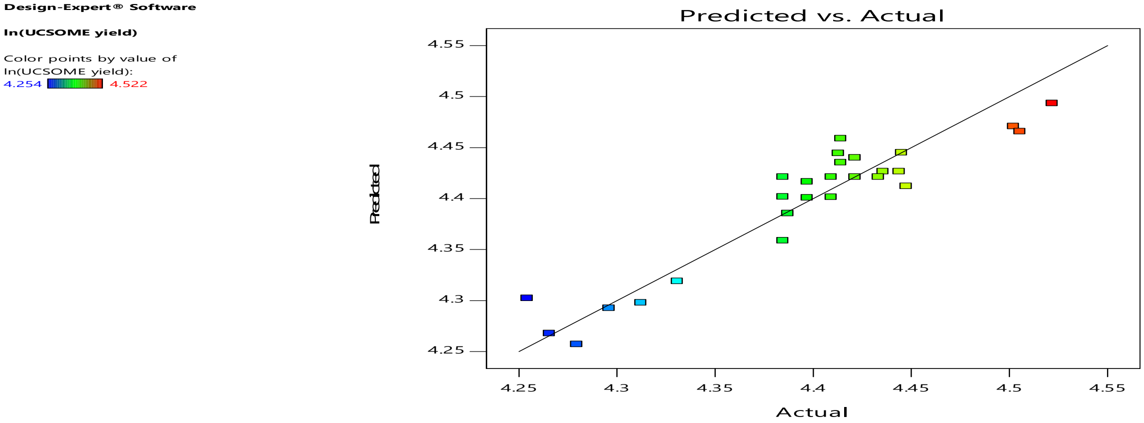

Figure 6: Predicted vs Actual plot

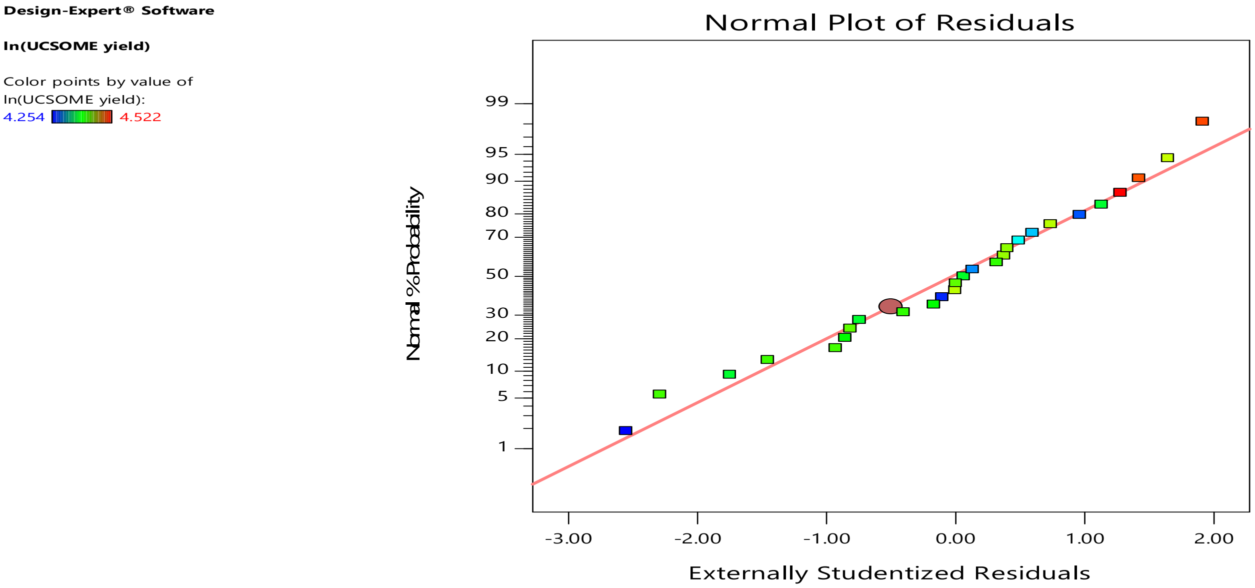

Figure 7: Normal plot of residuals

The experimental error that results from deducting the actual responses from the predicted responses is estimated using the normal plot of residuals. Following the estimation of all the unknown model parameters from the experimental data, the predicted response is determined using the selected model. The pattern closely resembles a straight line and there are no outliers, which indicates that the data set utilized for this experiment is normally distributed, according to the normal plot (Fig. 7).

3.3.Reusability of Calcined CaO _Blend derived catalyst

The economic viability of producing biodiesel on a large industrial scale is significantly influenced by the reusability and stability of CaO-based catalysts. Therefore, it was determined whether the calcined CaO catalyst could be reused. According to the findings, calcined CaO catalyst can be recycled up to six times. CaO catalyst that had been calcined steadily lost activity after being utilized more than five times (Fig. 9a). The biodiesel yield in each subsequent reuse cycle was 91.60 %, 85.50 %, 81.60 %, 78.60 %, 74.20 %, and 72.87 %. The loss of catalytic activity of calcined CaO catalyst may be ascribed to its structural changes. The SEM micrograph and EDX in Fig. 9b, show the agglomeration of other particles with the catalyst. Additionally, the availability of active catalyst sites for the reaction gradually declines due to the leaching of CaO to the other transesterification reactants. When comparing studies on the reusability of CaO catalyst in the literature, [62] after six recycle test runs, a 50 % biodiesel output was reported. [63] conducted three reusability experiments and recorded biodiesel yields in the first and third cycles of 86.14 % and 78.26 %, respectively. As a result, the reusability investigation shows that the CaO catalyst was stable for six transesterification reaction cycles, which is somewhat better than the results reported by [62].

3.4.Comparison of Calcined CaO _Blend derived Catalyst with the Commercial CaO

In this research, the Calcined CaO Blend derived catalyst activity was compared to that of calcined commercial CaO as well as to earlier research published in the literature. The results are shown in Table 10. In order to maintain consistency, UCSO with comparable physiochemical properties was tested using both the calcined commercial CaO and the calcined CaO-Blend. To get the highest yield of biodiesel, many factors including the methanol/oil ratio, catalyst wt. % (based on oil weight), reaction temperature, and reaction duration were changed. In the case of Calcined- CaO-Blend, it was observed that the maximum biodiesel yield of 92.00 % was obtained at a methanol/oil molar ratio of 10.80:1, 2.5 wt. % catalyst (based on oil weight), 60 °C reaction temperature, and 80 min of reaction duration. However, the calcined commercial CaO was able to produce a high biodiesel yield of 94.60 % using a methanol/oil molar ratio of 10.40:1, 2.5 wt. % catalyst (based on oil weight), 55 °C reaction temperature, and 80 min of reaction time. [64] found a maximum biodiesel yield of 95.00 % for the commercial CaO while transesterifying soybean oil at 65 °C with an 8 wt.% catalyst (based on oil weight), 12:1 methanol/oil molar ratio, and 3 hours of reaction time. Thus, employed efficiently, waste eggshells can operate as a solid catalyst for the transesterification of WFO (Waste Frying Oil), and their activity is on par with that of commercial CaO.

Table 8: Results of the Current Study in Comparison to Similar Studies

Optimum parameters	Feedstock	%Yield	References
Calcined-hydrated-dehydrated CaO-blend (from eggshell & coconut husk waste) 2.5 wt.%, 10:1, 60 °C, 80 min	Used cottonseed oil (UCSO)	92.10	This paper
Calcined-hydrated-dehydrated CaO (from eggshell) 5.0 wt.%, 12:1, 65 °C, 60 min	Waste Frying Oil (WFO)	94.52	[65]
KOH 1 wt%, 7:1, 40°C, 800 rpm	Shea biodiesel	92.16	[66]
NaOH 1.1 wt.%, 7:1, 60 °C, 600 rpm, 15 min	Used frying oil	88.80	[67]
Enzyme load (2 g), 12:1, 35°C,	Waste cooking oil	93.61	[68]
Silica sulfuric acid 5 %, 20:1, 373 K 8 hr	Cottonseed oil	97.86	[69]
CaO/KOH 7 wt.%, 12:1, 65 °C, 120 min	Waste cooking oil	87.17	[70]
CaO (from waste eggshell & rice husk) 1 wt%, 20:1, 60 °C, 120 min	Waste cooking oil	87.50	[71]

Table 9: Fit Summary Statistics for the Prediction of Suitable Model

Source	Sequential p-value	Lack of Fit p-value	Adjusted R^2	Predicted R^2	
Linear	1.81E-05	0.0737	0.6401	0.5282	Suggested
2FI	0.8607	0.0601	0.5713	0.1545	
Quadratic	0.039	0.0926	0.7385	0.3131	Suggested
Cubic	0.6351	0.0501	0.6987	-5.3453	Aliased

Table 10: Comparison of transesterification reaction conditions for different catalysts

		Optimum Transesterification Reaction Conditions				
The catalyst used Feedstock used	Feedstock used	Methanol/oil molar ratio	Catalyst wt.%	Temperature (°C)	Time (min)	Yield (%)
Calcined CaO_Blend	UCSO (this study)	10.8:01	2.5	60	80	92.10
Calcined Commercial CaO	UCSO (this study)	10.4:01	2.5	55	80	94.60
Commercial CaO	Soybean oil [64]	12:01	8	65	180	95.00

3.5.Fuel Properties of Biodiesel from Used Cottonseed Oil

Biodiesel has similar fuel characteristics to diesel fuels. Table 11 lists some of the fuel characteristics of methyl esters (biodiesels) produced from used cottonseed oil. The internal friction or flow resistance of an oil is measured by its viscosity. Methyl esters have fewer internal frictions than triglyceride molecules. Increasing the temperature of biodiesel causes its viscosity to decrease, allowing it to flow more easily. The most crucial characteristic of biodiesel is its viscosity, which has an impact on how fuel injection systems function, especially at low temperatures when the fuel fluidity is affected by the increase in viscosity. Biodiesel has viscosity close to diesel fuels. High viscosity leads to poorer atomization of the fuel spray and less accurate operation of the fuel injectors. The viscosity, density and flash point measurements of pure UCSO were 33–36 mm^2/s at 311 K, 911–916 kg/m^3 at 288 K and 504–510 K, respectively. The viscosities of UCSO methyl ester (UCSOME) were 3.6–3.7 mm^2/s and the density were 875–880 at 311 K. It is clear that the viscosity and density values of the UCSOME are significantly lower than those of the oil-based UCSO. Given that fuel injection equipment uses a volume metering system and that biodiesel has a higher density than conventional diesel, a slightly higher mass of fuel is delivered. While the flash points of the UCSOME are measured at 435–440 K as opposed to 504-510 K. Biodiesel often has a greater cetane number (CN) than regular diesel. The higher the CN, the longer the fatty acid carbon chains and the more saturated the molecules. Biodiesel produced from animal fats has a greater CN than biodiesel from vegetable oils [72]. From Table 11, it was found that the specific gravity of used cottonseed oil was decreased from 0.91 to 0.88 (33 % decrease) following transesterification, which is within the allowed limit. The saponification value of cottonseed oil was 188.32 mg/g while that of biodiesel was 165.87 mg/g. This suggests that the triglycerides of used cottonseed oil have a greater molecular weight of fatty acids (saturated and unsaturated). The comparison between this finding and the saponification values of palm oil (187–205), olive oil (185–187), and soy oil (187–193) is favourable [73]. The most crucial step in preventing adulteration is saponification. The idea that used cottonseed oil is edible is supported by the fact that it has an iodine value of 69.6 mg/g. For edible oil, the iodine value is less than 100 mg/g. In general, the degree of unsaturation and the propensity of the oil to develop oxidative rancidity increase with iodine value. The used cottonseed oil is a good source of raw material for biodiesel production even though the biodiesel has an iodine value of 104.7 mg/g, which is relatively high according to Europe EN 14214 specifications of iodine value. This is because the higher the iodine value, the more unsaturated double bonds are present in the molecular structure and the less viscous the biodiesel is [74]. Peroxide value is not stated in the biodiesel standards and is less suitable for monitoring oxidation [73], however, it affects the cetane number, a parameter listed in the fuel standard. Increase in cetane number and peroxide value result in a reduction in the ignition delay time [73].

Table 11: Fuel Characteristics of Used Cottonseed Oil (UCSO) and Used Cottonseed Oil Methyl Ester (UCSOME)

Fuel characteristics	**UCSO**	**UCSOME**
Viscosity (mm^2/s) (at 311 K)	33–36	3.6–3.7
Density (kg/m^3) (at 288 K)	911–916	875–880
Flash point (K)	504–510	435–440
Higher heating value (MJ/kg)	39.4–39.6	40.5–40.6
Distillation range (K)	528–628	
Cetane number	41.5–44.0	
Cloud point (K)	274–276	
Pour point (K)		257–259
Carbon residue (% by weight)		0.23–0.25
Ash content (% by weight)		0.008–0.010
Sulfur content (% by weight)		0.008–0.010
Acid value (mg KOH/g oil)		0.07–0.08
Specific gravity at 25°C		0.875
% Moisture content		
Kinematic viscosity (mm^2/s)		4.07
Saponification value (mgKOH/g)		204
Iodine value ($gI_2/100g$)		104.7
Fire point (°C)		215
Calorific value (MJ/kg)		

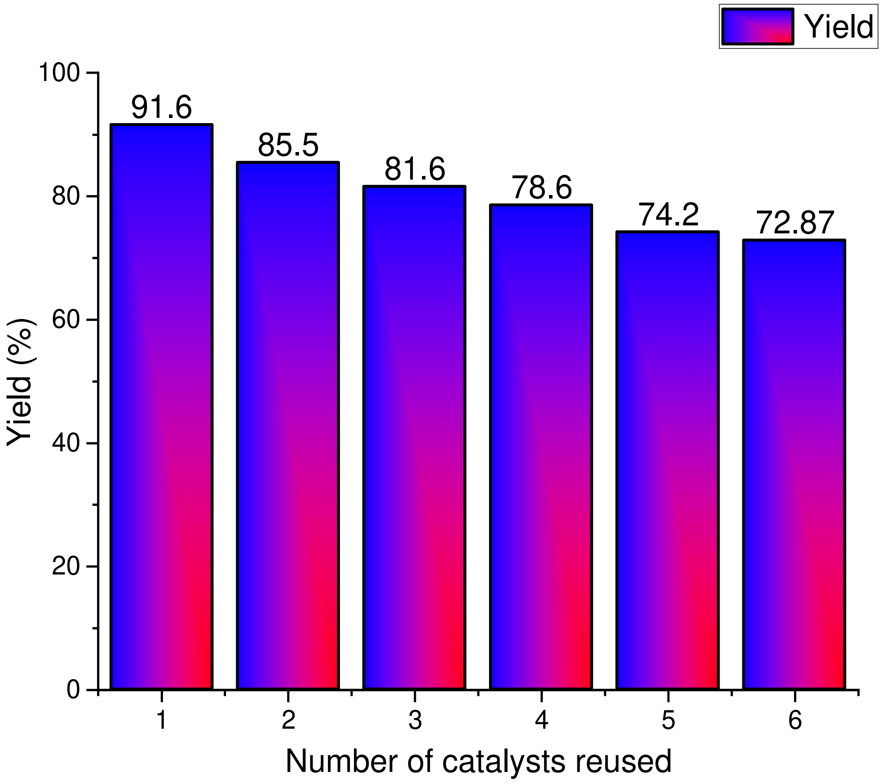

Figure 9a: Effect of Reusability of Calcined CaO_Blend on FAME Yield

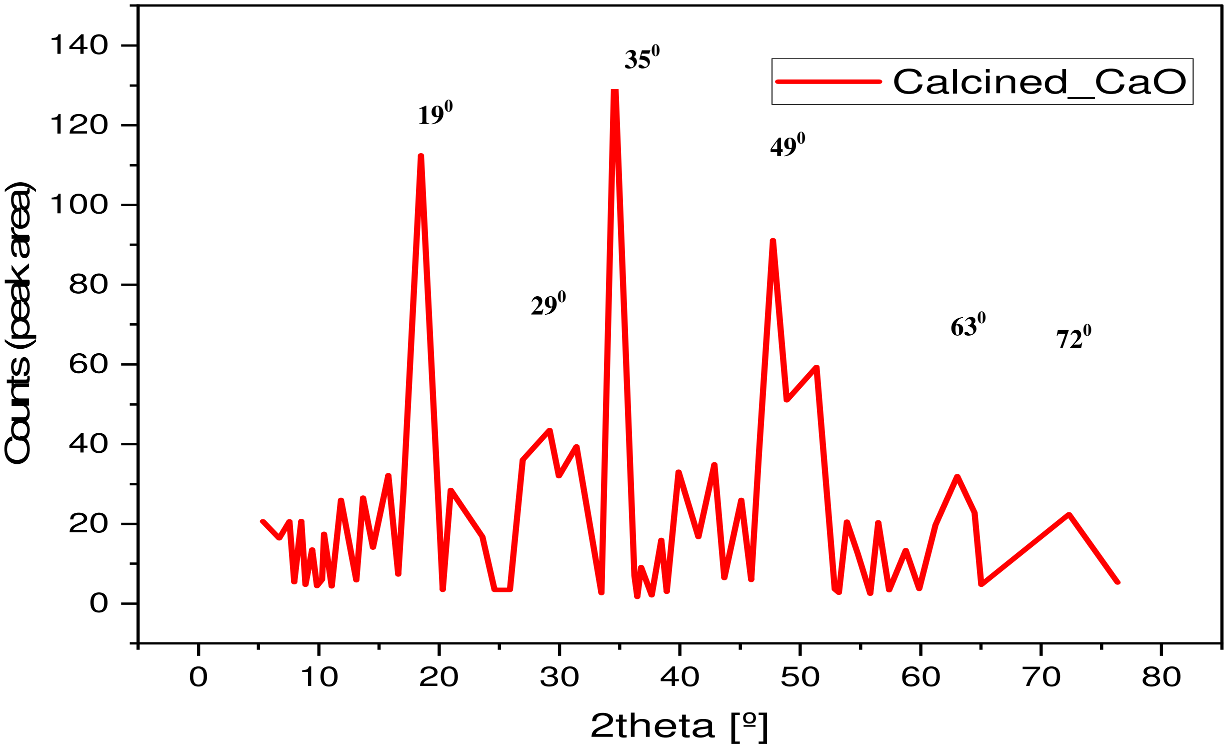

Figure 8: XRD Analysis of Calcined CaO_Blend Catalyst

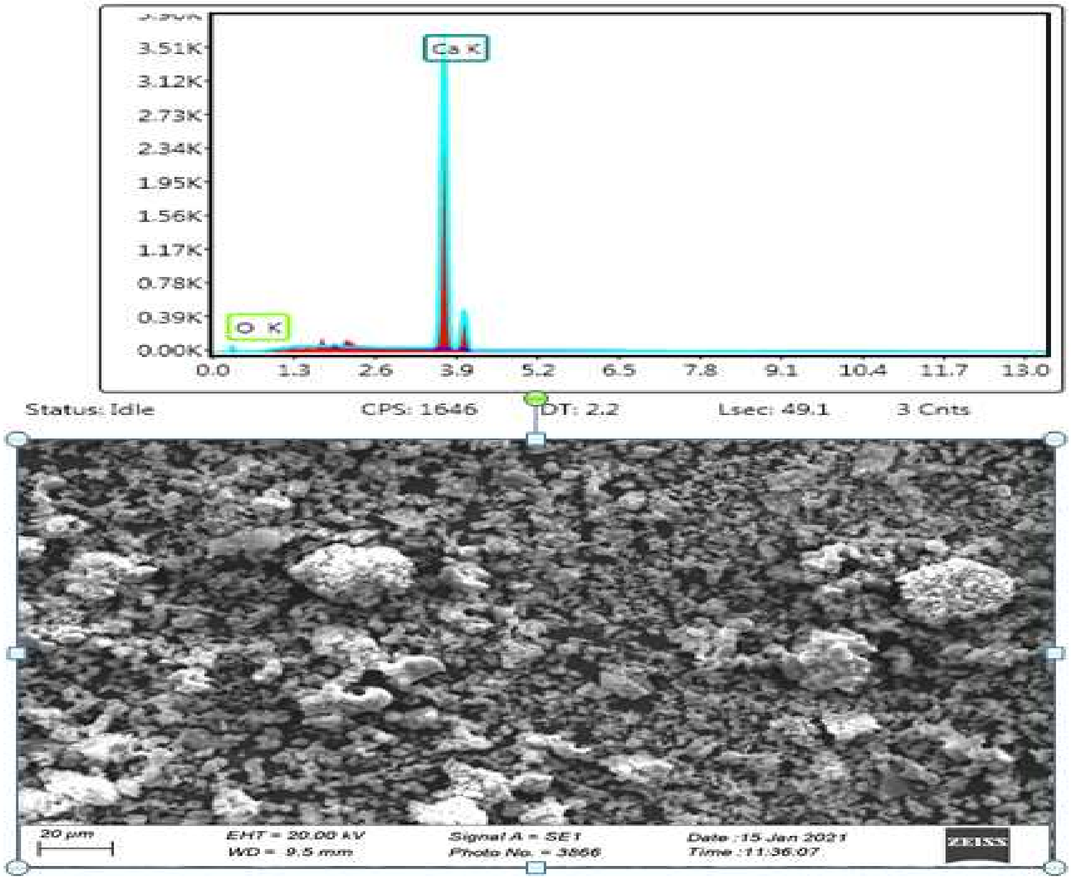

Figure 9b: Micrograph and EDX of Calcined CaO_Blend Catalyst

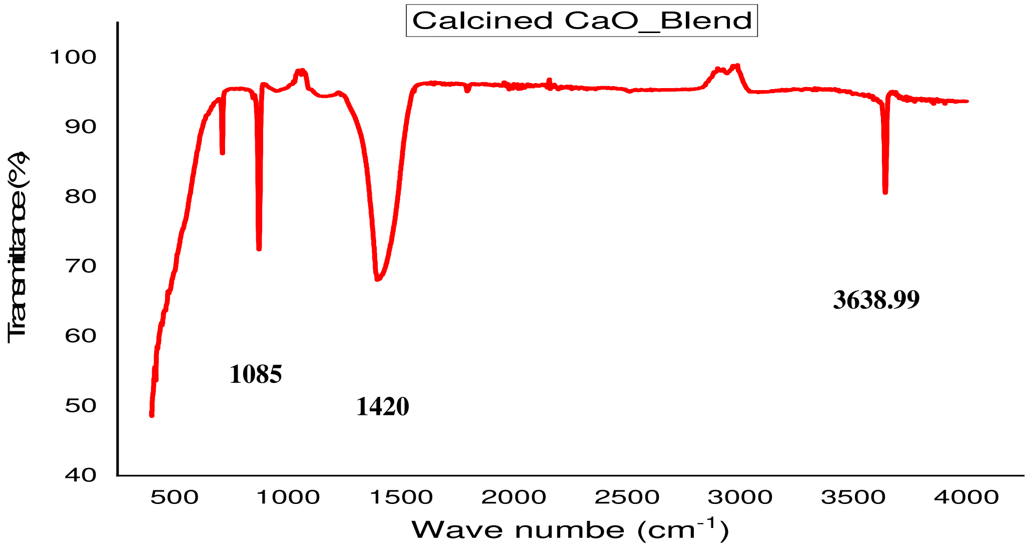

Figure 10: FTIR spectra of the Calcined CaO_Blend

3.6. Used Cotton Seed Oil (UCSO) and Used Cotton Seed Oil Methyl Ester (UCSOME) FTIR Analysis

The aliphatic CH_2 group symmetric stretching vibration is seen in strong absorption in the region of 2992 cm^{-1} as observed in the IR spectra of used cotton seed oil and used cotton seed oil methyl ester, respectively (Tables 11and 12; Figures 11 and 12). The large percentage of the linoleic acid group (33.43 %) could be the cause of this (Table 14 a & Table 15a). Similar results were observed with yellow oleander seed oil [75]. They also show absorbance at 1744 cm^{-1}, 1461 cm^{-1}, 1375 cm^{-1} 1159 cm^{-1}, 964 cm^{-1} and 723 cm^{-1}. However, there is a distinction between the spectra of the oils. Significant variations that are caused by the production of biodiesels can be shown in a comparative analysis of the FTIR peaks of the functional groups of the oils and their respective biodiesel. Biodiesel fatty acid methyl ester possesses a distinctive FTIR absorption of carbonyl (C=0) stretching vibrations near 1740-1744 cm^{-1} and C-O bending vibrations in the range of 1196 cm^{-1}. The characterization and quantification of FAMEs in biodiesel and used cotton seed oil by IR spectroscopy are based on this spectrum separation between the functional groups of used vegetable oils and their corresponding biodiesel [75]. The appearance of a signal at 1438 cm^{-1} (fig. 12), which corresponds to the deformation vibration of the methyl ester group (CO)-O-CH_3, present in the biodiesel spectrum but absent in the oil spectrum, served as an indicator of the influence of transesterification. A similar result was reported by [76][75]. The FTIR spectra of FAMEs also show the emergence of a signal at 964 cm^{-1} corresponding to CH_2 in the RCOCO- group present in the oil but absent in the FAMES, as well as a signal at 1170 cm^{-1} of the C-O group in the ester-controlled area.

Table 12: Interpretation of FTIR peaks (cm^{-1}) in Used Cotton Seed Oil (UCSO)

S/N	Peaks (cm^{-1})	Transmittance (%)	Remarks
1.	2922.2	57.481	Symmetric and asymmetric stretching vibrations of the aliphatic -CH_2 and -CH_3 groups
2.	2855.1	68.391	Symmetric and asymmetric stretching vibrations of the aliphatic -CH_2 and -CH_3 groups.
3.	1740.7	50.753	Double bond stretching -ester carbonyl functional group of the triglycerides
4.	1461.1	81.038	Long linear aliphatic chain of bounded and free fatty acids attached to triglyceride.
5.	1380.5	88.078	O-CH_2 present in triglyceride
6.	1249.5	81.339	C-H/C-N presence.
7.	1196.5	73.506	Fingerprint region -C-O stretching vibration of an ester group
8.	723.1	79.971	Overlapping of the CH_2 rocking vibration and the out-of-plane vibration of disubstituted olefins.

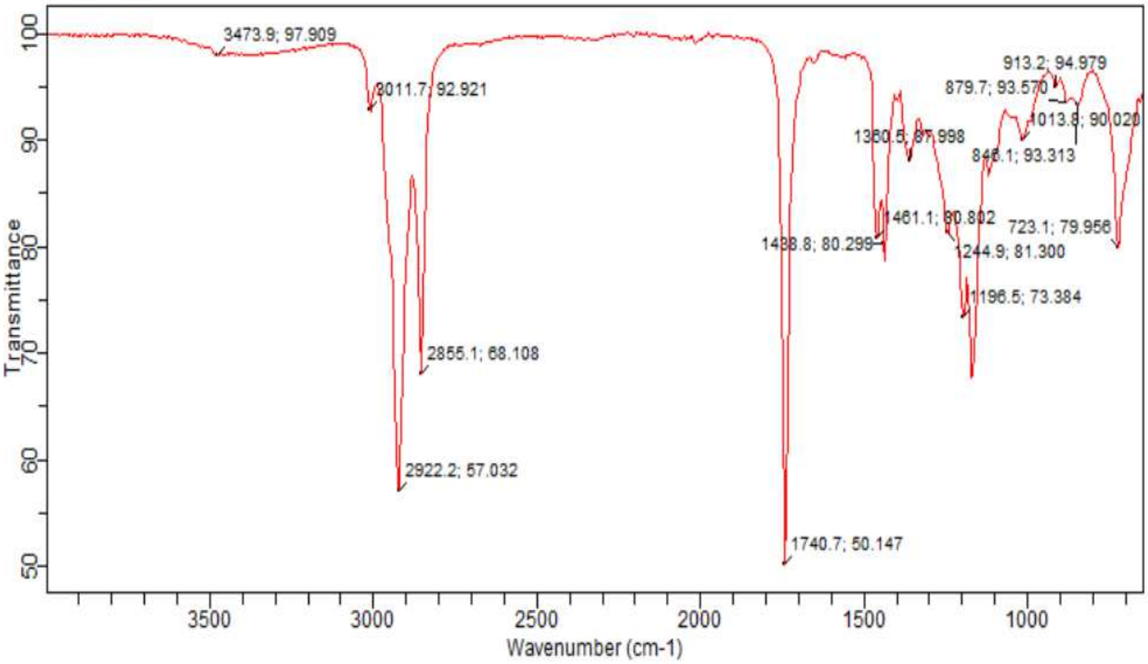

Figure 11: FTIR spectra of Used Cotton Seed Oil Methyl Ester (UCSOME)

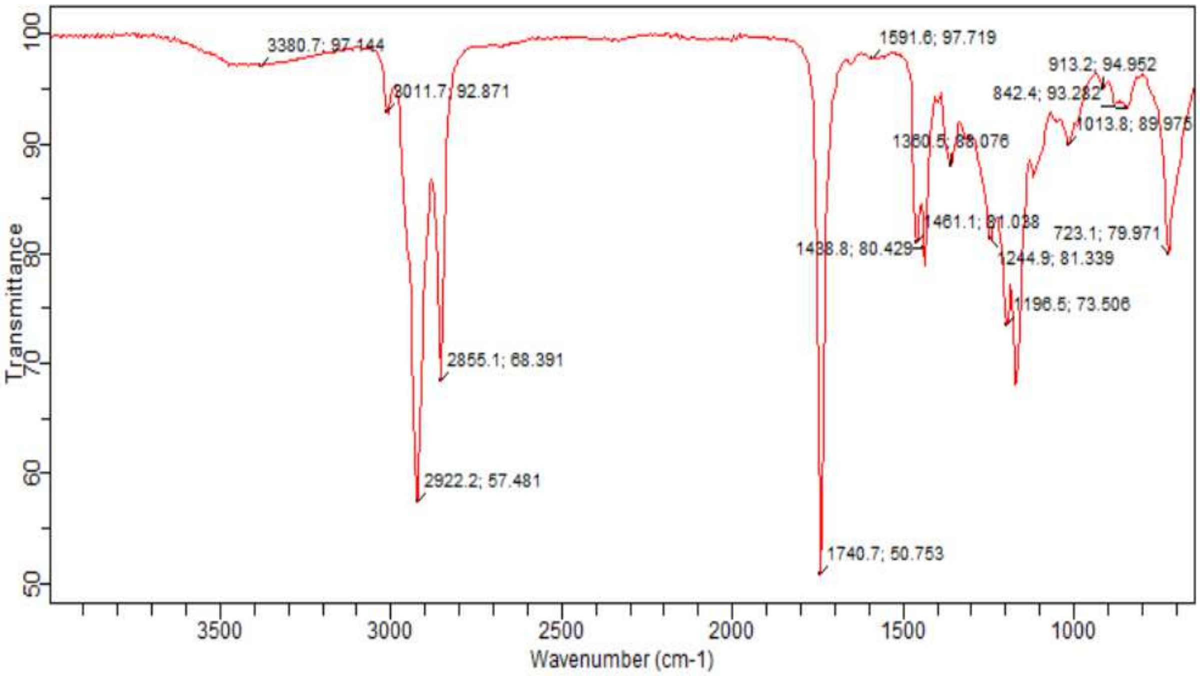

Figure 12: FTIR spectrum of Used Cotton Seed Oil (UCSO)

Table 13: Interpretation of FTIR peaks (cm^{-1}) in Used Cotton Seed Oil Methyl Ester (UCSOME)

S/N	Peaks (cm^{-1})	Transmittance (%)	Remark
1.	2922.2	57.032	Symmetric and asymmetric stretching vibrations of the aliphatic -CH_2 and -CH_3 groups
2.	2855.1	68.108	Symmetric and asymmetric stretching vibrations of the aliphatic -CH_2 and -CH_3 groups.
3.	1740.7	60.147	Double bond stretching -ester carbonyl functional group of the triglycerides
4.	1488.8	80.299	Long linear aliphatic chain of bounded and free fatty acids attached to triglyceride.
5.	1461.1	80.802	(CO) – O – CH_3 of methyl ester present
6.	1380.5	87.998	O-CH_2 present in triglyceride
7.	1244.9	81.300	C-H/C-N presence.
8.	1196.5	73.384	Fingerprint region -C-O stretching vibration of ester group in biodiesel
9.	1013.8	90.028	The C - O stretching of – O–CH_2 –C
10.	723.1	79.956	Overlapping of the CH_2 rocking vibration and the out-of-plane vibration of disubstituted olefins.

3.7.GC-MS Analysis

3.7.1.Used Cotton Seed Oil (UCSO) and Used Cotton Seed Oil Methyl Ester Fatty Acid Compositions (UCSOME)

The composition of fatty acids in UCSO is depicted in a gas chromatogram (figure 13), and their corresponding primary peaks and percentage compositions are listed in Tables 14a and b. Palmitic acid, linoleic acid, 11-Octadecenoic acid, Linoelaidic acid, stearic acid, and Lauric acid are the main fatty acids. The profile shows a high proportion of saturated and unsaturated fatty acids, including Lauric acid at 1.78 %, Stearic acid at 2.42 %, Linoelaidic acid at 7.69 %, 11-Octadecenoic acid at 16.04 %, Linoleic acid at 25.65 %, and Palmitic acid at 33.57 %. According to UCSO, which also shows a higher ratio of unsaturated than saturated fatty acids, linoleic acid is the unsaturated fatty acid and stearic and palmitic acid are the saturated fatty acids. Nearly all of the free fatty acids were in their methyl ester forms as a result of the methylation of the oil prior to the GC-MS investigation. The methyl derivatives contain molecular ions that are 14 mass units larger than those of the parent compounds, yet they nonetheless fragment in the same ways [77]. Thirty-four (34) different compounds, including methyl esters, butyl esters, steroids, dihydric alcohols, naphthalene, and phenolic compounds, are found in the UCSO according to the GC-MS study. The therapeutic benefits of UCSO are due to the large variety of substances present in it, including phytochemicals like Phytosterols, Tocopherols, Carotenoids, and Polyphenols. [78] insist that these phytochemicals can be used to make pharmaceuticals, cosmetics, and food since they have strong antibacterial, antioxidant, anti-proliferation, and anticancer effects. The GC-MS result shows the different concentrations of methyl esters of saturated and unsaturated fatty acids. However, linoleic acid comes in second place with 25.65 %, followed by 11-Octadecenoic acid with 16.04 %, and palmitic acid with 33.57 % in terms of relative percentage. Although polyunsaturated fatty acid methyl esters are susceptible to auto-oxidation, the relative oxidative and thermal stability of UCSO may have contributed to the saturation of palmitic and stearic acid. Compared to other polyunsaturated oils like mustard (94.27 %) and sunflower (88.39 %), UCSO is more stable [79]. The need for linoleic acid in the cosmetics sector is increasing [80]. When extracted, palmitic acid has a high economic value, and because it is unsaturated, it has been suggested that it can enhance the flow properties. Additionally, soap, cosmetics, and releasing agents are made with the sodium salt of palmitic acid [81]. According to reports, highly saturated oils have greater cloud points and cetane numbers and are more stable [82]. Chain length and the number of vacant bonds influence a number of biodiesel properties [83]. This finding aligns with other results in the literature [83]. Similar to this, Figure 4.14 Gas Chromatogram depicts the composition of fatty acids in UCSOME, while Tables 15a and b list their respective primary peaks and percentage compositions. The main fatty acids found in the methyl esters include palmitic acid, linoleic acid, lauric acid, myristic acid, stearic acid, and arachidic acid. The profile reveals a significant concentration of saturated fatty acids, with palmitic acid accounting for 29.64 %, linoleic acid for 33.43 %, lauric acid for 8.10 %, myristic acid for 6.67 %, stearic acid for 5.60 %, and arachidic acid for 1.17 %. With linoleic acid presenting the primary peak for the unsaturated fatty acid of the ester at 33.43 %, UCSOME reveals a larger amount of saturated fatty acids than unsaturated fatty acids. The principal fatty esters in UCSOME are Lauric acid (C12:0), Linoleic ester (19:2), Palmitic ester (C16:0), Stearic ester (C18:0), and Myristic acid (C14:0). Furthermore, the type of fatty acids plays a significant effect on the characteristics of biodiesel (Table 4.15b). The fatty acid content resembles that which was described by [84]. The large proportion of polyunsaturated fatty acids in UCSOME fuel increases the likelihood that it will experience auto-oxidation and rancidity, which will damage its storage property. With high cloud points and other fuel properties discovered in this sample, a larger level of polyunsaturated fatty acids in UCSOME was also imminent. The energy value of UCSOME was significantly increased by palmitic acid, a saturated fatty acid having a high heat of combustion of 38.905 MJ/kg. Fatty acid composition (92.00 %) of UCSOME is a strong indication that it can replace fossil fuel [85][86][87]. These findings closely align with earlier reports on the FA profile of CSO [88]. The majority of the polyunsaturated and some bulk saturated fatty acids that remain in the biodiesel are what give it its high viscosity. The biodiesel is primarily produced by transesterifying saturated and monounsaturated fatty acids. Because unsaturated fatty acids are easily oxidized, a higher concentration of them lowers fuel property. Unsaturated fatty acids like 18:1, 18:2, and 18:3 are generally less stable than saturated fatty acids like 16:0 or 18:0, which lowers the property of fuel. The results also show that transesterification produces methyl esters that are higher in saturated fatty acids than unsaturated fatty acids. Saturated fatty acids contribute to the high viscosity, high cetane number, and improved biodiesel stability.

Table 14a: Fatty Acid Composition of the UCSO and their Relative Percentages

Common Name	Symbol	Percentage of the total weight
Capric acid methyl ester	C11:0	0.23
Caprylic acid methyl ester	C09:0	1.05
Azelaaldehydic acid, methyl ester	C10:0	0.99
Myristic acid	C15:0	1.63
Lauric acid, methyl ester	C13:0	1.78
Methyl palmitoleate	C17:1	0.82
Palmitic acid, methyl ester	C17:0	33.57
Methyl 8-heptadecenoate	C18:1	0.17
Margaric acid methyl ester	C18:0	0.11
Linoleic acid, methyl ester	C19:2	25.65
11-Octadecenoic acid, methyl ester	C19:1	16.04
Methyl stearate	C19:0	2.42
Cyclopropaneoctanoic acid, 2-octyl, methyl ester	C20:0	0.35

7,10-Octadecadienoic acid, methyl ester	C19:2	0.15
Linolenic acid, methyl ester	C19:3	0.2
6,9-Octadecadienoic acid, methyl ester	C19:2	0.15
Linolelaidic acid, methyl ester	C19:2	0.70
Methyl 12-hydroxy-9-octadecenoate	C19:1	0.39
Arachidic acid methyl ester	C21:0	0.38
Behenic acid, methyl ester	C23:0	0.05
Linoelaidic acid	C19:4	7.69
Others		5.48

Table 14b: Major resolved peak areas of Used Cotton Seed Oil (UCSO) gas chromatogram and their suggested compound from NIST14 library

Peak No	Retention Time (min)	Area (%)	Compounds
6	22.78	1.78	Lauric acid, methyl ester
7	27.55	1.63	Myristic acid
10	30.70	33.57	Palmitic acid, methyl ester
11	31.11	2.32	n-Hexadecanoic acid
16	32.14	25.51	9,12-Octadecadienoic acid (Z,Z)-, methyl ester
17	32.18	16.04	11-Octadecenoic acid, methyl ester
18	32.31	2.42	Methyl stearate
19	32.49	7.69	Linoelaidic acid

Table 15a: Fatty acid composition of the UCSOME and their relative percentages

Common Name	Symbol	Percentage of the total weight
Myristic acid	C14:0	6.67
Linoleic acid, methyl ester	C19:2	33.43
Palmitic acid	C16:0	29.64
Lauric acid	C12:0	8.10
Caprylic acid methyl ester	C9:0	1.05
Methyl stearate	C19:0	5.60
Arachidic acid	C20:0	1.17
Capric acid methyl ester	C11:0	0.88
cis-10-Heptadecenoic acid, methyl ester	C18:1	0.73
Methyl 2-octylcyclopropene-1-octanoate	C12:1	0.64
Linoleic acid ethyl ester	C20:2	0.36
Docosanoic acid, methyl ester	C23:0	0.29
Pentadecanoic acid, methyl ester	C16:0	0.18
Methyl eladate	C19:1	0.15
Hexadecanoic acid, 14-methyl-, methyl ester	C18:0	0.26
Nonanoic acid, 9-oxo-, methyl ester	C10:0	0.14
Heneicosanoic acid, methyl ester	C22:0	0.12
Others		3.68

Table 15b: Major resolved peak areas of Used Cotton Seed Oil Methyl Ester (UCSOME) gas chromatogram and their suggested compound from NIST14 library

Peak No.	Retention Time (min)	Area (%)	Compounds
25	28.04	6.67	Myristic acid
27	30.89	29.64	Arachidic acid
32	32.31	33.43	Linoleic acid, methyl ester
33	32.99	5.60	Methyl stearate

36	33.75	1.17	Arachidic acid

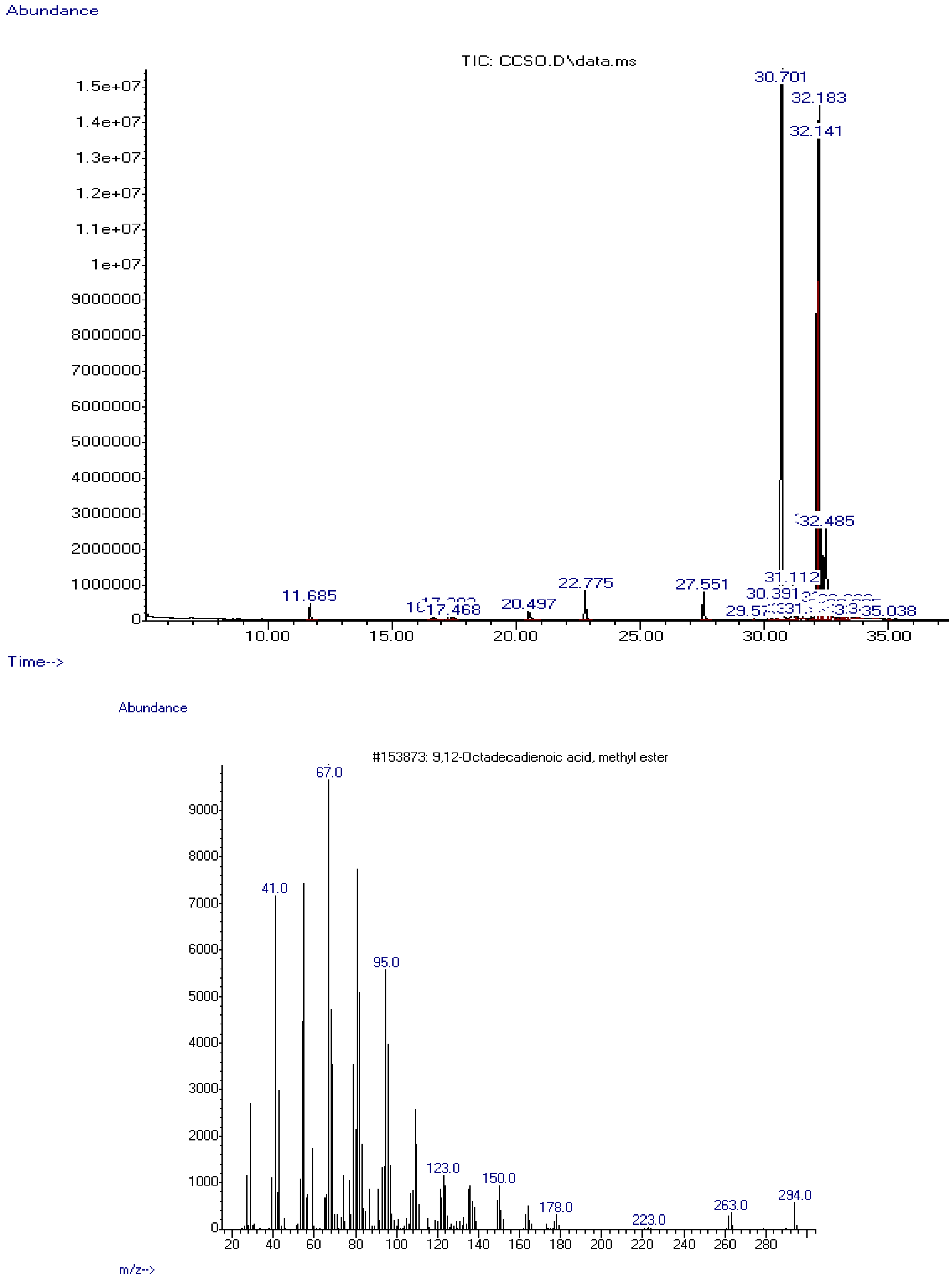

Figure 13: Gas chromatogram of some Used Cotton Seed Oil (UCSO)

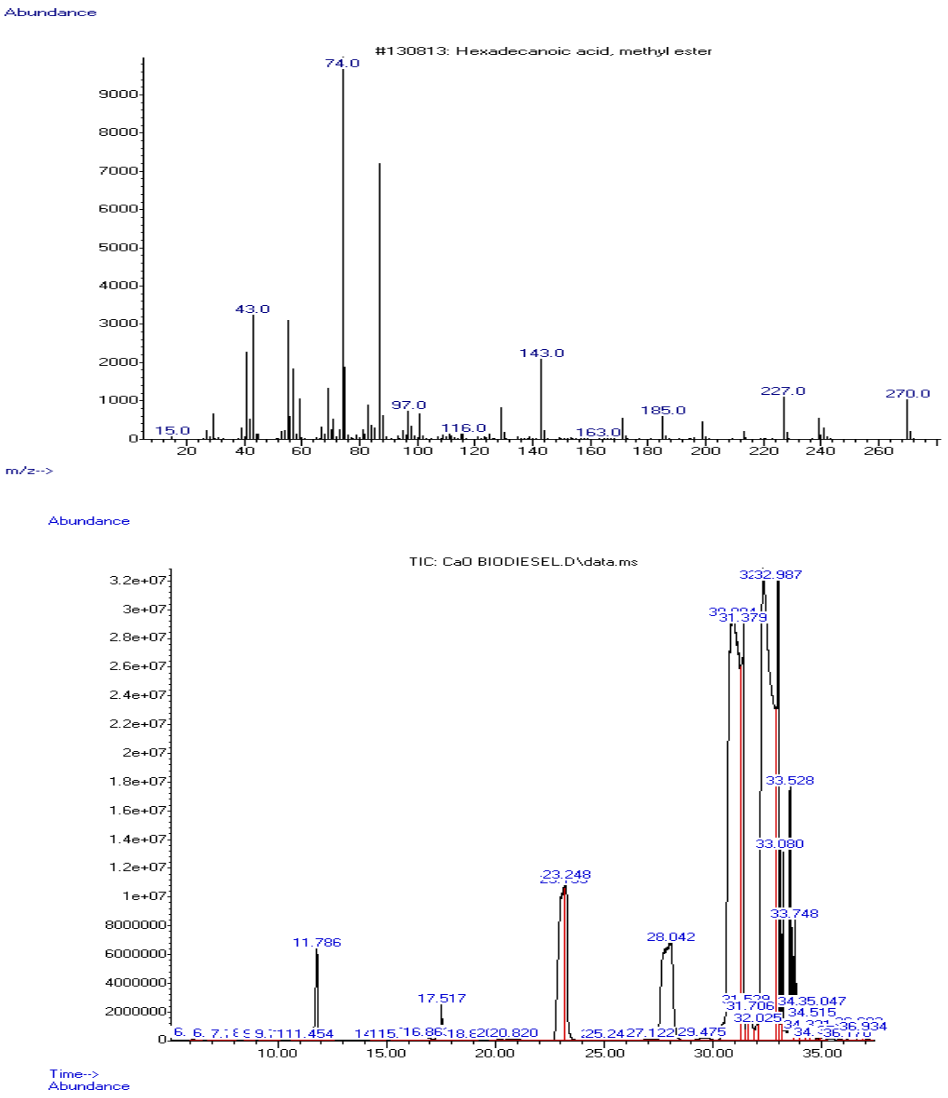

Figure 14: Gas chromatogram of Used Cotton Seed Oil Methyl Ester (UCSOME)

4.**Conclusion**

The Box-Behnken design was used to optimize the parameters using the response surface methodology. At a molar ratio of 1:10.80, a catalyst concentration of 2.5 wt. %, an 80-minute reaction period, and a reaction temperature of 60 °C, an optimum UCSOME yield of 92 % was obtained. The oil physicochemical characteristics and free fatty acid content make it appropriate for direct alkaline transesterification without acid pre-treatment, which makes production of fatty acid methyl ester inexpensive. At optimum circumstances for base catalyzed methanolysis reaction, it was discovered that the biodiesel yield of used cottonseed oil was high enough. The fatty acid methyl esters of UCSO displayed distinctive carbonyl (C=O) stretching vibrations at 1740.7 cm^{-1} in their FTIR spectra. The appearance of a signal at 1461.1 cm^{-1} for the (CO)-O-CH_3 group (a methyl ester group) in the biodiesel spectra served as evidence of the transesterification influence. Because of the C=O functional groups in fossil diesel, there are no such absorptions. Moreover, the GC-MS result revealed that UCSOME had 95 % saturated/unsaturated fatty esters, indicating the potential for high temperatures of combustion, consequently, a good alternative to fossil diesel. As a result, the extracted biodiesel quality metrics, including their density at 311 K (875–880), specific gravity (0.875 °C), flash point (435–440 K), dynamic viscosity (3.6–3.7 mm^2/s), cloud point (274–276 K), cetane number (41.5–44.0), and acid values (0.07–0.08mg KOH/g oil), were within the permitted ASTM standards for fuel grade biodiesels. The biodiesel yield in each subsequent reuse cycle was 91.60 %, 85.50 %, 81.60 %, 78.60 %, 74.20 %, and 72.87 %. The loss of catalytic activity of calcined CaO catalyst may be ascribed to its structural changes.

Acknowledgement

The management of the Multi-User Science Research Laboratory at Ahmadu Bello University in Zaria is gratefully acknowledged by the authors for providing the laboratory space necessary for this investigation.

References

[1] B. Reyes-Trejo *et al.*, “Annona diversifolia seed oil as a promising non-edible feedstock for biodiesel production,” *Ind Crops Prod*, vol. 52, pp. 400–404, 2014.

[2] A. Demirbas, “Progress and recent trends in biodiesel fuels,” *Energy Convers Manag*, vol. 50, no. 1, pp. 14–34, 2009.

[3] P. Tan, Z. Hu, D. Lou, and Z. Li, “Exhaust emissions from a light-duty diesel engine with Jatropha biodiesel fuel,” *Energy*, vol. 39, no. 1, pp. 356–362, 2012.

[4] [4] M. Shahabuddin, M. A. Kalam, H. H. Masjuki, M. M. K. Bhuiya, and M. Mofijur, “An experimental investigation into biodiesel stability by means of oxidation and property determination,” *Energy*, vol. 44, no. 1, pp. 616–622, 2012.

[5] [5] S. Ushakov, H. Valland, and V. Æsøy, “Combustion and emissions characteristics of fish oil fuel in a heavy-duty diesel engine,” *Energy Convers Manag*, vol. 65, pp. 228–238, 2013.

[6] [6] J.-J. Wang, Y.-Y. Jing, C.-F. Zhang, and J.-H. Zhao, “Review on multi-criteria decision analysis aid in sustainable energy decision-making,” *Renewable and sustainable energy reviews*, vol. 13, no. 9, pp. 2263–2278, 2009.

[7] [7] A. E. Atabani *et al.*, “A comparative evaluation of physical and chemical properties of biodiesel synthesized from edible and non-edible oils and study on the effect of biodiesel blending,” *Energy*, vol. 58, pp. 296–304, 2013.

[8] [8] X. Chen and M. Khanna, “Food vs. fuel: The effect of biofuel policies,” *Am J Agric Econ*, vol. 95, no. 2, pp. 289–295, 2013.

[9] [9] Y. A. Elsheikh, “Preparation of *Citrullus colocynthis* biodiesel via dual-step catalyzed process using functionalized imidazolium and pyrazolium ionic liquids for esterification step,” *Ind Crops Prod*, vol. 49, pp. 822–829, 2013.

[10] [10] M. A. Kalam, M. G. Saifullah, H. H. Masjuki, M. Husnawan, and T. M. I. Mahlia, “PAH and other emissions from coconut oil blended fuels,” 2008.

[11] [11] A. S. Silitonga, H. H. Masjuki, T. M. I. Mahlia, H. C. Ong, and W. T. Chong, “Experimental study on performance and exhaust emissions of a diesel engine fuelled with Ceiba pentandra biodiesel blends,” *Energy Convers Manag*, vol. 76, pp. 828–836, 2013.

[12] Y. K. Ong and S. Bhatia, “The current status and perspectives of biofuel production via catalytic cracking of edible and non-edible oils,” *Energy*, vol. 35, no. 1, pp. 111–119, 2010.

[13] A. S. Ramadhas, S. Jayaraj, and C. Muraleedharan, “Use of vegetable oils as IC engine fuels a review,” *Renew Energy*, vol. 29, no. 5, pp. 727–742, 2004.

[14] M. Tariq, S. Ali, and N. Khalid, “Activity of homogeneous and heterogeneous catalysts, spectroscopic and chromatographic characterization of biodiesel: A review,” *Renewable and Sustainable Energy Reviews*, vol. 16, no. 8, pp. 6303–6316, 2012.

[15] M. Kouzu, T. Kasuno, M. Tajika, Y. Sugimoto, S. Yamanaka, and J. Hidaka, “Calcium oxide as a solid base catalyst for transesterification of soybean oil and its application to biodiesel production,” *Fuel*, vol. 87, no. 12, pp. 2798–2806, 2008.

[16] Y. M. Sani, W. M. A. W. Daud, and A. R. A. Aziz, “Solid acid-catalyzed biodiesel production from microalgal oil The dual advantage,” *J Environ Chem Eng*, vol. 1, no. 3, pp. 113–121, 2013.

[17] [17] A. Takagaki *et al.*, “Esterification of higher fatty acids by a novel strong solid acid,” *Catal Today*, vol. 116, no. 2, pp. 157–161, 2006.

[18] [18] Y. M. Sani, W. M. A. W. Daud, and A. R. A. Aziz, “Activity of solid acid catalysts for biodiesel production: a critical review,” *Appl Catal A Gen*, vol. 470, pp. 140–161, 2014.

[19] [19] S. Niju, K. M. Meera, S. Begum, and N. Anantharaman, “Modification of egg shell and its application in biodiesel production,” *Journal of Saudi Chemical Society*, vol. 18, no. 5, pp. 702–706, 2014.

[20] [20] N. Viriya-empikul, P. Krasae, B. Puttasawat, B. Yoosuk, N. Chollacoop, and K. Faungnawakij, “Waste shells of mollusk and egg as biodiesel production catalysts,” *Bioresour Technol*, vol. 101, no. 10, pp. 3765–3767, 2010.

[21] [21] S. Niju, K. M. M. S. Begum, and N. Anantharaman, “Enhancement of biodiesel synthesis over highly active CaO derived from natural white bivalve clam shell,” *Arabian Journal of Chemistry*, vol. 9, no. 5, pp. 633–639, 2016.

[22] [22] Y. Eswararao, S. Niju, K. M. Meera Sheriffa Begum, N. Anantharaman, and S. Malik Raj, “Transesterification of jatropha oil using a mixture of natural shells as solid catalyst,” *Biofuels*, vol. 7, no. 4, pp. 345–351, 2016.

[23] [23] J. Boro, A. J. Thakur, and D. Deka, “Solid oxide derived from waste shells of *Turbonilla striatula* as a renewable catalyst for biodiesel production,” *Fuel Processing Technology*, vol. 92, no. 10, pp. 2061–2067, 2011.

[24] [24] P.-L. Boey, G. P. Maniam, and S. Abd Hamid, “Biodiesel production via transesterification of palm olein using waste mud crab (Scylla serrata)

shell as a heterogeneous catalyst," *Bioresour Technol*, vol. 100, no. 24, pp. 6362–6368, 2009.

[25] [25] P.-L. Boey, G. P. Maniam, S. A. Hamid, and D. M. H. Ali, "Crab and cockle shells as catalysts for the preparation of methyl esters from low free fatty acid chicken fat," *J Am Oil Chem Soc*, vol. 88, no. 2, pp. 283–288, 2011.

[26] [26] Y. Y. Margaretha, H. S. Prastyo, A. Ayucitra, and S. Ismadji, "Calcium oxide from Pomacea sp. shell as a catalyst for biodiesel production," *International Journal of Energy and Environmental Engineering*, vol. 3, no. 1, pp. 1–9, 2012.

[27] [27] S. Jairam, P. Kolar, R. Sharma-Shivappa, J. A. Osborne, and J. P. Davis, "KI-impregnated oyster shell as a solid catalyst for soybean oil transesterification," *Bioresour Technol*, vol. 104, pp. 329–335, 2012.

[28] [28] S. L. Lee, Y. C. Wong, Y. P. Tan, and S. Y. Yew, "Transesterification of palm oil to biodiesel by using waste obtuse horn shell-derived CaO catalyst," *Energy Convers Manag*, vol. 93, pp. 282–288, 2015.

[29] [29] M. Kaur and A. Ali, "Lithium ion impregnated calcium oxide as nano catalyst for the biodiesel production from karanja and jatropha oils," *Renew Energy*, vol. 36, no. 11, pp. 2866–2871, 2011.

[30] [30] E. Modiba, C. Enweremadu, and H. Rutto, "Production of biodiesel from waste vegetable oil using impregnated diatomite as heterogeneous catalyst," *Chin J Chem Eng*, vol. 23, no. 1, pp. 281–289, 2015.

[31] [31] S. Sadhukhan and U. Sarkar, "Production of biodiesel from Crotalaria juncea (Sunn-Hemp) oil using catalytic trans-esterification: Process optimisation using a factorial and Box–Behnken design," *Waste Biomass Valorization*, vol. 7, no. 2, pp. 343–355, 2016.

[32] [32] H. Hamze, M. Akia, and F. Yazdani, "Optimization of biodiesel production from the waste cooking oil using response surface methodology," *Process Safety and Environmental Protection*, vol. 94, pp. 1–10, 2015.

[33] [33] A. S. Bharadwaj, M. Singh, S. Niju, K. M. M. S. Begum, and N. Anantharaman, "Biodiesel production from rubber seed oil using calcium oxide derived from eggshell as catalyst–optimization and modeling studies," *Green Processing and Synthesis*, vol. 8, no. 1, pp. 430–442, 2019, doi: https://doi.org/10.1515/gps-2019-0011.

[34] [34] B. Yoosuk, P. Udomsap, B. Puttasawat, and P. Krasae, "Modification of calcite by hydration–dehydration method for heterogeneous biodiesel production process: the effects of water on properties and activity," *Chemical Engineering Journal*, vol. 162, no. 1, pp. 135–141, 2010.

[35] [35] J. Van Gerpen, "Cetane number testing of biodiesel," in *Proceedings, third liquid fuel conference: liquid fuel and industrial products from renewable resources*, 1996, pp. 197–206.

[36] [36] S. C. Sekhar *et al.*, "Biodiesel production process optimization from Pithecellobium dulce seed oil: Performance, combustion, and emission analysis on compression ignition engine fuelled with diesel/biodiesel blends," *Energy Convers Manag*, vol. 161, pp. 141–154, 2018, Accessed: Aug. 30, 2022. [Online]. Available: https://doi.org/10.1016/j.enconman.2018.01.074

[37] [37] H. T. Nguyen, C. L. Walker, and E. A. Walker, *A first course in fuzzy logic*. CRC press, 2018.

[38] [38] C. De Blasio, "Biodiesel," in *Fundamentals of Biofuels Engineering and Technology*, Springer, 2019, pp. 253–265.

[39] [39] F. Bagheban Shahri and A. Niazi, "Synthesis of modified maghemite nanoparticles and its application for removal of Acridine Orange from aqueous solutions by using Box-Behnken design," *J Magn Magn Mater*, vol. 396, pp. 318–326, 2015, doi: 10.1016/j.jmmm.2015.08.054.

[40] [40] M. C. Sekhar, B. P. Reddy, K. Mallikarjuna, G. Shanmugam, C.-H. Ahn, and S.-H. Park, "Synthesis, characterization, and analysis of enhanced photocatalytic activity of Zr-doped TiO_2 nanostructured powders under UV light," *Mater Res Express*, vol. 5, no. 1, p. 15024, 2018.

[41] [41] G. A. Miraculas, N. Bose, and R. E. Raj, "Process parameter optimization for biodiesel production from mixed feedstock using empirical model," *Sustainable Energy Technologies and Assessments*, vol. 28, pp. 54–59, 2018.

[42] [42] R. Foroutan, R. Mohammadi, H. Esmaeili, F. M. Bektashi, and S. Tamjidi, "Transesterification of waste edible oils to biodiesel using calcium oxide@ magnesium oxide nanocatalyst," *Waste Management*, vol. 105, pp. 373–383, 2020.

[43] [43] Y. H. Tan, M. O. Abdullah, C. Nolasco-Hipolito, and Y. H. Taufiq-Yap, "Waste ostrich-and chicken-eggshells as heterogeneous base catalyst for biodiesel production from used cooking oil: Catalyst characterization and biodiesel yield performance," *Appl Energy*, vol. 160, pp. 58–70, 2015.

[44] [44] K. Seffati, B. Honarvar, H. Esmaeili, and N. Esfandiari, "Enhanced biodiesel production from chicken fat using $CaO/CuFe_2O_4$ nanocatalyst and its combination with diesel to improve fuel properties," *Fuel*, vol. 235, pp. 1238–1244, 2019.

[45] [45] Z. Teimouri, A. Salem, and S. Salem, "Microwave-assisted for clean and rapid fabrication of highly efficient magnetically separable activated carbon from agriculture shells for low grade industrial corn syrup decoloration: A novel strategy for impregnation of ternary catalytic composite," *Food and Bioproducts Processing*, vol. 116, pp. 78–88, 2019.

[46] [46] S. Niju, J. Indhumathi, K. M. M. S. Begum, and N. Anantharaman, "Tellina tenuis: a highly active environmentally benign catalyst for the transesterification process," *Biofuels*, vol. 8, no. 5, pp. 565–570, 2017.

[47] [47] B. J. Burnett, A. Giles, A. L. Anderson, T. Darger, and E. Walker, "Rapid Determination of Gold during Plating Operations by Portable X-Ray Fluorescence," *Am J Analyt Chem*, vol. 5, no. 17, p. 1178, 2014.

[48] [48] F. M. Almutairi, "Biopolymer Nanoparticles: A Review of Prospects for Application as Carrier for Therapeutics and Diagnostics.," *International Journal of Pharmaceutical Research & Allied Sciences*, vol. 8, no. 1, 2019.

[49] [49] S. M. Bahshwan, S. O. A. Rabah, and A. M. Turkistani, "A Comparative Study of The Effect of Crude and Nanoparticles *Costus Speciosus* On Testicular Damage Associated to Experimentally Induced Type 2 Diabetes." Pharmacophore, 2019.

[50] [50] N. Mozayyeni, A. Morsali, M. R. Bozorgmehr, and S. A. Beyramabadi, "Structural and mechanistic studies of γ-Fe2O3 nanoparticle as troxacitabine drug nanocarrier," *Arch Pharm Pract*, vol. 10, no. 1, pp. 31–37, 2019.

[51] [51] H. Babaei, A. A. Sepahy, K. Amini, and S. Saadatmand, "The Effect of Titanium Dioxide Nanoparticles Synthesized by *Bacillus tequilensis* on clb Gene Expression of Colorectal Cancer-causing Escherichia coli," *Arch Pharm Pract*, vol. 11, no. 1, pp. 22–31, 2020.

[52] [52] J. Gupta and M. Agarwal, "Preparation and characterizaton of CaO nanoparticle for biodiesel production," in *AIP conference proceedings*, 2016, vol. 1724, no. 1, p. 20066.

[53] [53] E. Bet-Moushoul, K. Farhadi, Y. Mansourpanah, A. M. Nikbakht, R. Molaei, and M. Forough, "Application of CaO-based/Au nanoparticles as heterogeneous nanocatalysts in biodiesel production," *Fuel*, vol. 164, pp. 119–127, 2016.

[54] [54] A. O. Ayeni, M. O. Daramola, P. T. Sekoai, O. Adeeyo, M. J. Garba, and A. A. Awosusi, "Statistical modelling and optimization of alkaline peroxide oxidation pretreatment process on rice husk cellulosic biomass to enhance enzymatic convertibility and fermentation to ethanol," *Cellulose*, vol. 25, no. 4, pp. 2487–2504, 2018.

[55] [55] V. Makareviciene, V. Skorupskaite, D. Levisauskas, V. Andruleviciute, and K. Kazancev, "The optimization of biodiesel fuel production from microalgae oil using response surface methodology," *Int J Green Energy*, vol. 11, no. 5, pp. 527–541, 2014.

[56] [56] N. Tshizanga, E. F. Aransiola, and O. Oyekola, "Optimisation of biodiesel production from waste vegetable oil and eggshell ash," *S Afr J Chem Eng*, vol. 23, no. 1, pp. 145–156, 2017.

[57] [57] S. Niju, K. M. M. Sheriffa Begum, and N. Anantharaman, "Preparation of biodiesel from waste frying oil using a green and renewable solid catalyst derived from egg shell," *Environ Prog Sustain Energy*, vol. 34, no. 1, pp. 248–254, 2015.

[58] [58] J. K. Ratnadhariya and S. A. Channiwala, "Three zone equilibrium and kinetic free modeling of biomass gasifier–a novel approach," *Renew Energy*, vol. 34, no. 4, pp. 1050–1058, 2009.

[59] [59] M. Atapour, H.-R. Kariminia, and P. M. Moslehabadi, "Optimization of biodiesel production by alkali-catalyzed transesterification of used frying oil," *Process Safety and Environmental Protection*, vol. 92, no. 2, pp. 179–185, 2014.

[60] [60] N. Ghaffari Saeidabad *et al.*, "A Review on Catalysts Development for Steam Reforming of Biodiesel Derived Glycerol; Promoters and Supports," *Catalysts*, vol. 10, no. 8, p. 910, 2020.

[61] [61] A. Lee, N. Chaibakhsh, M. B. A. Rahman, M. Basri, and B. A. Tejo, "Optimized enzymatic synthesis of levulinate ester in solvent-free system," *Ind Crops Prod*, vol. 32, no. 3, pp. 246–251, 2010.

[62] [62] Y. H. Taufiq-Yap, H. V Lee, M. Z. Hussein, and R. Yunus, "Calcium-based mixed oxide catalysts for methanolysis of Jatropha curcas oil to biodiesel," *Biomass Bioenergy*, vol. 35, no. 2, pp. 827–834, 2011.

[63] [63] L. Marques Correia, J. A. Cecilia, E. Rodríguez-Castellón, C. L. Cavalcante, and R. S. Vieira, "Relevance of the physicochemical properties of calcined quail eggshell (CaO) as a catalyst for biodiesel production," *J Chem*, vol. 2017, 2017.

[64] [64] X. Liu, H. He, Y. Wang, S. Zhu, and X. Piao, "Transesterification of soybean oil to biodiesel using CaO as a solid base catalyst," *Fuel*, vol. 87, no. 2, pp. 216–221, 2008.

[65] [65] S. Niju, R. Rabia, K. S. Devi, M. N. Kumar, and M. Balajii, "Modified Malleus Malleus shells for biodiesel production from waste cooking oil: An optimization study using box–behnken design," *Waste Biomass Valorization*, vol. 11, no. 3, pp. 793–806, 2020.

[66] [66] E. O. Ajala, F. Aberuagba, A. M. Olaniyan, M. A. Ajala, and M. O. Sunmonu, "Optimization of a two stage process for biodiesel production from shea butter using response surface methodology," *Egyptian Journal of Petroleum*, vol. 26, no. 4, pp. 943–955, 2017.

[67] [67] D. Y. C. Leung and Y. Guo, "Transesterification of neat and used frying oil: optimization for biodiesel production," *Fuel processing technology*, vol. 87, no. 10, pp. 883–890, 2006.

[68] [68] S. A. Razack and S. Duraiarasan, "Response surface methodology assisted biodiesel production from waste cooking oil using

encapsulated mixed enzyme," *Waste management*, vol. 47, pp. 98–104, 2016.

[69] [69] K. A. Shah, K. C. Maheria, and J. K. Parikh, "Effect of reaction parameters on the catalytic transesterification of cottonseed oil using silica sulfuric acid," *Energy Sources, Part A: Recovery, Utilization, and Environmental Effects*, vol. 38, no. 10, pp. 1470–1477, 2016.

[70] [70] S. Oko, I. Syahrir, and M. Irwan, "The Utilization of CaO Catalyst Impregnated With KOH In Biodiesel Production From Waste Cooking Oil," *J Teknol*, vol. 82, no. 2, 2020.

[71] [71] N. S. Lani, N. Ngadi, N. Y. Yahya, and R. Abd Rahman, "Synthesis, characterization and performance of silica impregnated calcium oxide as heterogeneous catalyst in biodiesel production," *J Clean Prod*, vol. 146, pp. 116–124, 2017.

[72] [72] M. Balat, "Current alternative engine fuels," *Energy Sources*, vol. 27, no. 6, pp. 569–577, 2005.

[73] [73] J. Mohammed, U. Edith, S. J. Atuman, and A. A. Aboje, "Production and characterization of biodiesel from jatropha oil and neem oil," 2012.

[74] [74] D. O. Onukwuli, L. N. Emembolu, C. N. Ude, S. O. Aliozo, and M. C. Menkiti, "Optimization of biodiesel production from refined cotton seed oil and its characterization," *Egyptian Journal of Petroleum*, vol. 26, no. 1, pp. 103–110, 2017.

[75] [75] Y. A. Dallatu, E. B. Agbaji, and V. O. Ajibola, "The influence of physicochemical characteristics of a non-edible oil of yellow oleander seed on its fuel properties," *Bayero Journal of Pure and Applied Sciences*, vol. 10, no. 2, pp. 283–291, 2017.

[76] [76] N. G. Siatis, A. C. Kimbaris, C. S. Pappas, P. A. Tarantilis, and M. G. Polissiou, "Improvement of biodiesel production based on the application of ultrasound: monitoring of the procedure by FTIR spectroscopy," *J Am Oil Chem Soc*, vol. 83, no. 1, pp. 53–57, 2006.

[77] [77] J. Omowanle, R. J. Ayo, J. Habila, J. Ilekhaize, and E. A. Adegbe, "Physico-Chemical and GC-MS Analysis of Some Selected Plant Seed Oils; Castor, Neem and Rubber Seed Oils," *FUW Trends in Sci. and Techn. J*, vol. 3, no. 2, pp. 644–651, 2018.

[78] [78] P. W. Mwaurah *et al.*, "Physicochemical characteristics, bioactive compounds and industrial applications of mango kernel and its products: A review," *Compr Rev Food Sci Food Saf*, vol. 19, no. 5, pp. 2421–2446, 2020.

[79] [79] C. Dorni, P. Sharma, G. Saikia, and T. Longvah, "Fatty acid profile of edible oils and fats consumed in India," *Food Chem*, vol. 238, pp. 9–15, 2018.

[80] [80] H. Darmstadt, C. Roy, S. Kaliaguine, S. J. Choi, and R. Ryoo, "Surface chemistry of ordered mesoporous carbons," *Carbon N Y*, vol. 40, no. 14, pp. 2673–2683, 2002.

[81] [81] A. A. Warra, F. Sheshi, H. S. Ayurbami, and A. Abubakar, "Physico-chemical, GC-MS analysis and cold saponification of canary melon (Cucumis melo) seed oil," *Trends in Industrial Biotechnology Research*, vol. 1, no. 1, pp. 10–17, 2015.

[82] [82] R. Piloto-Rodríguez, Y. Sánchez-Borroto, M. Lapuerta, L. Goyos-Pérez, and S. Verhelst, "Prediction of the cetane number of biodiesel using artificial neural networks and multiple linear regression," *Energy Convers Manag*, vol. 65, pp. 255–261, 2013.

[83] [83] G. Knothe, R. O. Dunn, and M. O. Bagby, "Biodiesel: the use of vegetable oils and their derivatives as alternative diesel fuels," in *ACS symposium series*, 1997, vol. 666, pp. 172–208.

[84] [84] J. O. Alademeyin and J. O. Arawande, "OF SCIENTIFIC AND Physicochemical properties and fatty acid composition of crude and processed *Adenopus breviflorus Benth* seed oil," vol. 51, no. 3, pp. 159–166, 2016.

[85] [85] W. Institute, *Biofuels for transport: global potential and implications for sustainable energy and agriculture*. Earthscan, 2012.

[86] [86] C. Beaudoin-Chabot, L. Wang, A. V Smarun, D. Vidović, M. S. Shchepinov, and G. Thibault, "Deuterated polyunsaturated fatty acids reduce oxidative stress and extend the lifespan of C. elegans," *Front Physiol*, vol. 10, p. 641, 2019.

[87] [87] M. I. Oseni, S. E. Obetta, and F. V Orukotan, "Evaluation of fatty acids profile of ethyl esters of yellow oleander and groundnut oils as biodiesel feedstock," *American Journal of Scientific and Industrial Research*, vol. 3, no. 2, pp. 62–68, 2012.

[88] [88] U. Rashid, F. Anwar, and G. Knothe, "Evaluation of biodiesel obtained from cottonseed oil," *Fuel Processing Technology*, vol. 90, no. 9, pp. 1157–1163, 2009, doi: 10.1016/j.fuproc.2009.05.016.